https://doi.org/10.5194/bg-2023-173
Preprint. Discussion started: 4 October 2023

Biogeosciences
Discussions
Open Access
EGU

Structural complexity and benthic metabolism: resolving the links between carbon cycling and biodiversity in restored seagrass meadows

Theodor Kindeberg[1*], Karl M. Attard[2,3], Jana Hüller[1], Julia Müller[1], Cintia O. Quintana[2,4], Eduardo Infantes[5]

[1]Department of Biology, Lund University, Sölvegatan 37, 223 62, Lund, Sweden
[2]Department of Biology, University of Southern Denmark, 5230, Odense M, Denmark
[3]Danish Institute for Advanced Study, University of Southern Denmark, 5230, Odense M, Denmark
[4]SDU Climate Cluster, University of Southern Denmark, 5230, Odense M, Denmark
[5]Department of Biological and Environmental Sciences, University of Gothenburg, 451 78, Kristineberg, Sweden

[*]Correspondence: theo.kindeberg@gmail.com

Abstract. Due to large losses of seagrass meadows worldwide, restoration is proposed as a key strategy for increasing coastal resilience and recovery. The emergence of a seagrass meadow is anticipated to substantially increase biodiversity and enhance benthic metabolism through increased primary productivity and respiration. Yet, open questions remain regarding the metabolic balance of aging seagrass meadows and the roles benthic communities of the seagrass ecosystem play in overall metabolism.

To address these questions, we investigated a chronosequence of bare sediments, adjacent *Zostera marina* meadows of three and seven years since restoration and a natural meadow located within a high-temperate marine embayment in Gåsö, Sweden. We combined continuous measurements of O_2 fluxes using underwater eddy covariance with dissolved inorganic carbon (DIC) and O_2 fluxes from benthic chambers during the productive season (July). Based on the ratio between O_2 and DIC, we obtained site-specific photosynthetic and respiratory quotients from which we could convert eddy covariance fluxes to DIC. We assessed benthic diversity parameters as potential drivers of metabolic flux variability.

We observed high rates of gross primary productivity (GPP) spanning -18–-82 mmol DIC m^{-2} d^{-1} which increased progressively with meadow age. Community respiration (CR) mirrored the GPP trend, and all meadows were net heterotrophic (GPP < |CR|), ranging from 16–28 mmol DIC m^{-2} d^{-1}. While autotrophic biomass did not increase with meadow age, macrophyte diversity did, elucidating potential effects of niche complementarity on community metabolism. These observations provide insights into how community composition and meadow development relate to ecosystem functioning and highlight potential tradeoffs between carbon uptake and biodiversity.

https://doi.org/10.5194/bg-2023-173
Preprint. Discussion started: 4 October 2023

1. Introduction

Climate change and concurrent biodiversity loss has motivated restoration of natural ecosystems that can contribute to climate change mitigation, adaptation and at the same time strengthen local biodiversity. One such ecosystem is seagrass meadows, which has suffered substantial losses worldwide during the last century (Mckenzie et al., 2020; Waycott et al., 2009). Due to its foundational role in structuring benthic communities, high productivity and ability to sequester large amounts of carbon, restoring previously lost meadows has been proposed as a low-regret option to address both the climate crisis and the biodiversity crisis concomitantly (Unsworth et al., 2022; Orth et al., 2020; Duarte et al., 2013; Gattuso et al., 2018). Nevertheless, few studies have assessed whether both these goals are mutually attainable within the same restoration projects, or if there are trade-offs between biodiversity conservation and carbon sequestration.

The mechanisms through which a seagrass meadow modifies carbon flows are manifold, influencing both import, export and burial of autochthonous (i.e. seagrass biomass) and allochthonous (i.e. organic matter from other sources) carbon (Duarte and Krause-Jensen, 2017). While sedimentation of allochthonous carbon is largely a passive process ultimately governed by local hydrodynamics, autochthonous carbon sequestration is coupled to the productivity of the seagrass meadow and is thus a function of its metabolic fluxes on timescales ranging from minutes to years (Duarte and Cebrian, 1996; Smith and Hollibaugh, 1993; Smith and Key, 1975). Seagrass community metabolism is comprised of gross primary productivity (GPP) and community respiration (CR) constituted by autotrophic and heterotrophic respiration. The balance between GPP and CR on a daily basis reflects the net metabolism, hereafter termed net community productivity (NCP = GPP - |CR|). The magnitude and direction of GPP, CR and NCP determine all subsequent carbon flows whereby a positive NCP (net autotrophy) equals the net carbon fixed available for remineralization, burial or export (Duarte and Krause-Jensen, 2017). Contrarily, if NCP is negative, the meadow is respiring more organic carbon than is fixed and relies on external or historic inputs of organic matter to sustain metabolism. Empirically assessing community metabolism is thus imperative to constrain a carbon budget and infer the potential net effect of a seagrass meadow on carbon sequestration.

The vast majority of metabolism studies in seagrass ecosystems to date are based on oxygen fluxes (Ward et al., 2022). Converting these fluxes into carbon currency often relies on assuming a constant stoichiometric 1:1 ratio between oxygen and dissolved inorganic carbon (O_2:DIC) fluxes which may significantly under- or overestimate actual metabolism (e.g. Turk et al., 2015; Barron et al., 2006; Duarte et al., 2010). For marine sediments, this ratio has been estimated to range between 0.8 – 1.2 on annual timescales (Glud, 2008 and references therein) but the variability is poorly constrained and likely higher in seagrass systems and on shorter timescales (Trentman et al., 2023; Turk et al., 2015). The discrepancy from a 1:1 ratio between benthic oxygen and DIC fluxes can stem from a wide range of processes, including anaerobic sediment processes, nitrate assimilation, photorespiration and differences in solubility and air-sea gas exchange rates between O_2 and CO_2 (Weiss, 1970; Trentman et al., 2023). In seagrasses, storage in tissues and transport of oxygen to roots and subsequent radial oxygen loss (ROL) can also contribute to deviations from the theoretical 1:1 relation (Ribaudo et al., 2011; Borum et al., 2007; Berg et al., 2019). Assessing carbon cycling in seagrass meadows without characterizing the marine carbonate chemistry system can thus lead to erroneous conclusions regarding their role in carbon cycling and ultimately their climate change mitigation potential.

https://doi.org/10.5194/bg-2023-173
Preprint. Discussion started: 4 October 2023


Biogeosciences
Discussions
Open Access
EGU

Despite the growing number of seagrass restoration projects worldwide, assessments of the effect on benthic metabolism are lacking. To our knowledge, the only research effort that has specifically addressed benthic metabolism in restored seagrass was carried out in Virginia Coast Reserve, USA (Rheuban et al., 2014a), where a large-scale *Zostera marina* restoration project commenced in 2001 (Mcglathery et al., 2012). Rheuban et al. (2014a) employed a chronosequence approach comprised of a bare site and two stages of development since restoration (5 years and 11 years) and measured benthic metabolism on diel and seasonal timescales. The authors found that GPP and |CR| increased up to 25- and 10-fold, respectively with meadow age and this was consistent through seasons. Yet, NCP was similar, and slightly negative, between the bare site and the oldest restored meadow on an annual basis, despite the vast differences in autotrophic biomass between the two sites (Rheuban et al., 2014a). Notably, summer metabolism revealed a net autotrophic state in the five-year-old meadow (NCP), whereas the older, mature meadow (11yr) had much higher metabolic fluxes and net heterotrophy on the order of about -50 mmol O_2 m^{-2} d^{-1} (Hume et al., 2011; Rheuban et al., 2014a).

Although GPP often substantially increases during summer in temperate seagrass meadows, so does CR to a similar extent (Ward et al., 2022). Consequently, despite large seasonal variability in photosynthesis and respiration, the metabolic state (NCP) is often relatively stable on an annual basis, granted there are no major ecosystem shifts. Interannual variability of NCP has been related to seagrass die-off and recovery episodes (Berger et al., 2020), and seagrass phenology typically dictate fluxes and metabolic state on intra-annual timescales (e.g. Champenois and Borges, 2012; Rheuban et al., 2014a). However, a seagrass meadow is comprised of several components that all contribute to community metabolic fluxes. Aside from the seagrass itself, these include primary producers such as macro- and microalgae and heterotrophic organisms ranging from macrofauna to bacteria. Together, these make up the fluxes of O_2 and DIC measured in the overlying water column by methods such as aquatic eddy covariance, benthic chambers or open water mass balance. Isolating fluxes deriving from a single meadow component is difficult *in situ*, although promising efforts have been made at estimating the role of benthic fauna in meadow metabolism (Rodil et al., 2021; Rodil et al., 2019a; Rodil et al., 2019b). When planting seagrass with the stated goals of obtaining both a carbon sink and a biodiversity hotspot, it is essential to understand the relationship between these two and over what timescales it may change as a meadow develops. It is therefore necessary to employ a holistic approach and assess biogeochemical and biodiversity parameters in tandem across multiple stages of seagrass growth. Importantly, both autotrophic and heterotrophic components of biodiversity are relevant as they are expected to have contrasting effects on metabolism.

The overarching goal of this study was thus to assess how metabolic fluxes and biodiversity change as the benthic environment evolves from bare sediment to a mature seagrass meadow following active seagrass restoration. We hypothesized that in an early stage, autotrophic biomass is dominating but total biomass is relatively low, resulting in small diel variability in metabolic fluxes and a net autotrophic state. As the meadow grows, fauna colonizes and organic matter builds up, the system goes toward a balanced metabolic state as |CR| increases relative to GPP. Finally, when the meadow has reached maturity, CR and GPP are tightly coupled in a system with high turnover and a balanced NCP.

To test these hypotheses, we utilized a chronosequence of four stages of seagrass development since restoration located within the same sheltered bay. We employed non-invasive, high-resolution aquatic eddy covariance (EC) in conjunction with benthic chamber incubations (BC). From this we could simultaneously record fluxes of O_2 and carbonate chemistry parameters from which we could evaluate daily metabolic fluxes of both

https://doi.org/10.5194/bg-2023-173
Preprint. Discussion started: 4 October 2023

117 oxygen and carbon. Additionally, we investigated multiple features of taxonomic and functional diversity of both
118 macrophytes and benthic fauna and assessed surficial sediment carbon stocks to infer short-term effects of
119 seagrass restoration on carbon cycling and biodiversity.

https://doi.org/10.5194/bg-2023-173
Preprint. Discussion started: 4 October 2023

2. Methods

2.1 Site description

The study took place between July 4–20, 2022 in the island of Gåsö (58.2325, 11.3984) located at the mouth of the Gullmar fjord on the west coast of Sweden (Fig. 1). The bay of Gåsö is a semi-enclosed bay spanning ~0.3 km^2 with two narrow inlets and outlets.

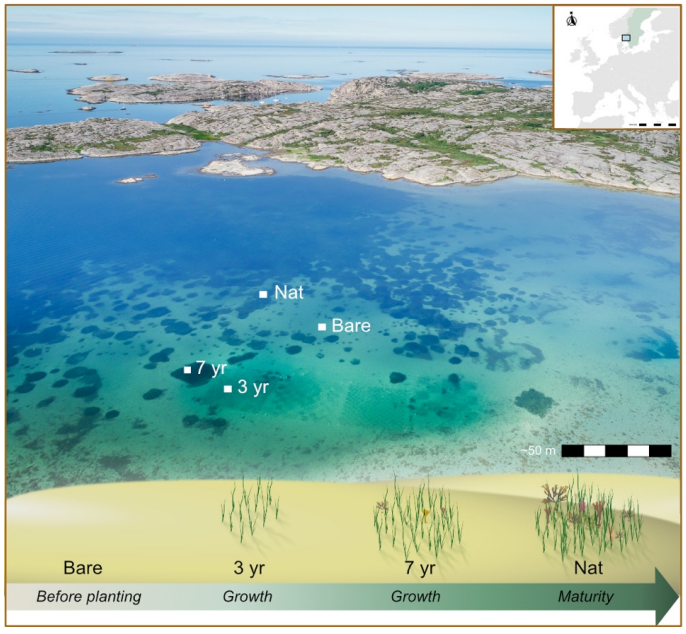

Figure 1 Aerial view and seagrass development stages after restoration. a) Map showing study location and drone image of Gåsö bay. b) Schematic illustration of seagrass meadow development in the four sites Bare, 3 yr, 7 yr and Nat which represent different stages of meadow development as indicated by the arrow and text in italics.

The benthos consists of a natural, continuous eelgrass (*Z. marina*) meadow and large patches interspersed with bare sediment occurring between 1–4 m depth (Fig. 1; Huber et al., 2022). In 2015 and 2019, as part of the seagrass restoration program ZORRO (www.gu.se/en/research/zorro), two plots of *Z. marina* were planted at the same depth (~2 m), using the same planting methodology (single-shoot) and shoot density (16 shoots m^{-2}) (Gagnon et al., 2023). These plots thus provided a chronosequence of seagrass meadow ages spanning three and seven years since planting, while the bare sediment area and the natural meadow corresponded to a 'before' state and a mature meadow, respectively. The part of the natural meadow we sampled was estimated to have been naturally colonized by meadow expansion 13–15 years ago (E. Infantes, pers. obs.). Altogether, this yielded four sites within 100 m distance from each other representing four different stages in the development of a seagrass meadow (Fig. 1). Importantly, the validity of applying a chronosequence methodology to investigate age-related differences in seagrass metabolism relies on assumptions that the sites compared experienced similar abiotic conditions after planting and during sampling. Utilizing adjacent sites within a semi-enclosed bay addresses most of those matters but to further control assumptions, we monitored *in situ* flow velocity, photosynthetic active radiation (PAR),

https://doi.org/10.5194/bg-2023-173
Preprint. Discussion started: 4 October 2023

142 temperature, salinity and wind conditions during all deployments and assessed the variation explained by each
143 variable using linear mixed effects models (see below).
144

145 **2.2 Benthic fluxes**

146 **2.2.1 Aquatic eddy covariance (EC)**

147 The EC system (Berg et al., 2003) consisted of a stainless-steel tripod frame with an acoustic doppler velocimeter
148 (ADV Vector, Nortek) and a fast-responding oxygen microsensor (430 UHS, Pyroscience GmbH) programmed
149 to log data continuously at 16 Hz from co-located measurements of velocity and oxygen concentration. In addition,
150 two PAR sensors (LI-192, RBR) were mounted to the frame where one was facing upwards to record incident
151 light and one was directed downwards to record reflected light. This made it possible to calculate the fraction of
152 absorbed light (*fAPAR*) during deployments. Dissolved oxygen optodes (miniDOT, PME and U26 HOBO, Onset)
153 were mounted on the leg of the frame and recorded ambient oxygen concentration within the canopy at 1 min
154 intervals. In addition, a salinity sensor (U24 HOBO, Onset), a turbidity sensor (RBRsolo, RBR) and two light
155 intensity loggers (HOBO Pendant MX, Onset) were located on the frame recording at 1 min intervals.

156 **2.2.2 Benthic chambers (BC)**

157 Benthic incubation chambers consisted of acrylic cylinders (inner diameter = 12.45 cm, length = 65 cm) with a
158 custom-made motor running a propeller to mix the water within the chamber and avoid build-up of vertical
159 concentration gradients. We employed pilot tests with dye injection in the laboratory and field to ensure sufficient
160 mixing and during incubations, chambers were inserted approximately 20 cm into the sediment. We used
161 transparent (n=3) and opaque (n=3) chambers to simulate day (photosynthesis and respiration) and night
162 (respiration only), respectively. Upon deployment, chambers were left with lids off for about 30 mins to allow for
163 suspended sediment to settle.
164 We drew discrete samples of seawater at onset and termination of each incubation using two 50 mL
165 syringes attached to 30 cm Tygon® tubing, inserted through a closable sampling port in the chamber lid. We
166 immediately analyzed seawater in the syringes for pH and dissolved oxygen (DO). pH was measured using an
167 InLab Micro pH electrode with a FiveGo handheld pH meter (Mettler Toledo). The electrode was calibrated both
168 using a two-point calibration with standard buffers (pH 7 and 10, Mettler Toledo) at the onset and termination of
169 the field campaign and calibrated to certified Tris buffer in synthetic seawater (Dr. A. Dickson, SIO) in the
170 beginning and end of each sampling day. This was done to account for the effect of salinity and to yield values
171 on the total hydrogen ion scale (pH_T). We measured salinity using a conductivity probe connected to a pH/cond
172 340i multimeter (WTW).
173 We measured DO using a fiberoptic oxygen sensor coupled to a FireSting® GO2 oxygen meter
174 (PyroScience). A temperature probe was also connected to the FireSting® to record temperature during each
175 measurement. Seawater from the syringes was then filtered through 0.45 µm Minisart® sterile syringe filters
176 (Sartorius) and stored in 50 mL Falcon tubes on ice. Upon return to the laboratory, we placed samples for TA in
177 a dark container at 4 ºC whereas samples for inorganic nutrients and DOC were frozen (-20 ºC) immediately until
178 subsequent laboratory analyses.

https://doi.org/10.5194/bg-2023-173
Preprint. Discussion started: 4 October 2023

We determined TA by open-cell potentiometric titration using an 888 Titrando system with an Ecotrode plus pH electrode (Metrohm). Samples (40–50 g) were titrated with prepared 0.05 M HCl in ~0.6 mol kg^{-1} NaCl, corresponding to the ionic strength obtained from the mean salinity of the samples. Accuracy and precision (-1.65±3.76 µmol kg^{-1}) were determined using certified reference material (CRM, batch 200, n=8) provided by Dr. Andrew Dickson at Scripps Institution of Oceanography, San Diego.

We analyzed dissolved inorganic nitrogen (NH_4-N and NO_3-N) using Flow Injection Analysis on a FIA Star 5000 analyzer (FOSS) and phosphate (PO_4-P) using ion chromatography on an 861 Advanced Compact IC (Metrohm). We analyzed dissolved organic carbon (DOC) and total nitrogen (TN) using a V-CPH Total Organic Carbon analyzer (Shimadzu).

We calculated DIC using the package *seacarb* in *R* (Gattuso et al., 2022) with measured values of pH_T and TA in conjunction with in situ temperature, salinity, pressure and NH_4^+ as input parameters. We used dissociation constants K_1^* and K_2^* from Lueker et al. (2000). We also calculated the saturation state of $CaCO_3$ mineral form aragonite ($\Omega_{Ar}=[Ca^{2+}][CO_3^{2-}]/K_{sp}^*$) from each sample using *seacarb*. All solute concentrations were calculated to µmol kg^{-1}, using *in situ* pressure, temperature and salinity data.

Using incubations with discrete measurements to assess flux rates assumes that concentrations change linearly with time. We verified this assumption *ex situ* by bringing an intact chamber core from the natural meadow into the laboratory. The chamber was placed in a large water bath with running seawater and prior to each incubation, the chamber was saturated with oxygen by bubbling compressed air. We ran multiple dark incubations with continuous logging of dissolved oxygen and temperature (FireSting® GO2) combined with multiple discrete measurements of pH (n=4) and TA (n=2).

2.3 Community components

2.3.1 Macrophytes

We evaluated seagrass shoot density by placing a 0.25 m x 0.25 m frame randomly in ten areas of each site and counting seagrass shoots in subareas of 0.016 m^2 (n=10 per site). In addition, we collected seagrass shoots using a mesh net bag attached to a closable aluminum frame (opening area = 0.1156 m^2, n=3 per site). From these samples, we measured aboveground biomass, shoot density, number of reproductive shoots, leaf length, and number of leaves per shoot. We also assessed the taxa and biomass of macrophytes other than seagrass (e.g. red and brown macroalgae). We dried biomass samples at 60 ºC for 72 hours and values are reported as dry mass (g m^{-2}).

2.3.2 Benthic fauna

We targeted infauna and epifauna separately where we collected epifauna from the mesh net bag samples described above (mesh size ~ 0.2 mm, n=3 per site). This approach allows for capturing the entire community by which cores captures infauna and slow-moving epifauna and the mesh net approach captures fast-moving and larger epifauna. For infauna, we collected sediment cores using polycarbonate cylinders (inner diameter: 7.4 cm, length: 33 cm, 20 cm depth, n=6 per site) for determination of infauna and seagrass belowground biomass. Upon return to the laboratory, samples were sieved (0.5 mm) and fixed in 95 % ethanol for subsequent counting and species identification. Fauna was identified to lowest taxonomic level possible.

https://doi.org/10.5194/bg-2023-173
Preprint. Discussion started: 4 October 2023

2.3.3 Sediment properties

In addition to the sediment cores used for infauna, we collected three additional sediment cores from each site to determine sediment properties. These cores were stored upright and immediately brought back to the lab and sliced into sections at 2, 4, 6, 8, 12, 16 cm depth. We used the top 0–2 cm section for determination of chlorophyll *a*, water content, dry bulk density (DBD, g cm^{-3}) and porosity (see below). After removing visible root fragments and shells, we dried remaining sections at 60 ºC for 72 hours, homogenized with a pestle and mortar and subsamples (5 mL) analyzed for organic matter content using loss on ignition (4 hours at 520 ºC). Subsamples from the top 0–2 cm sediment layer (n=12) were also analyzed for particulate organic carbon (POC), particulate inorganic carbon (PIC) and total nitrogen (TN) using a Vario MAX TN elemental analyzer (Elementar). We pre-treated samples with HCl to remove carbonates and PIC was obtained by subtracting POC from total carbon (TC). We obtained a linear relationship between OM and POC (POC=0.47*OM-0.88; R^2=0.84, p<0.001) which we used as a conversion factor to convert remaining OM values to POC and thereby obtain POC values for all core slices. We calculated carbon density for each slice between 0–12 cm by multiplying POC with surface DBD and integrated across 0–12 cm to obtain the organic carbon stock (POC_{stock}, g m^{-2}) in the upper 12 cm of sediment. Using only DBD values for the top 0–2 cm introduces uncertainty in our depth-integrated POC_{stock} estimates but a previous study by Dahl et al. (2023) from the same area showed similar DBD values from 0–11 cm (mean 0.43±0.15 g cm^{-3}) that were consistent with sediment depth.

2.3.4 Chlorophyll a

We collected samples for sediment surface chlorophyll *a* to serve as a proxy for microphytobenthos. From each sediment core, we used a cutoff 5-mL syringe (Ø=12 mm) to collect 2 mL sediment from the surface layer. This was repeated three times for each core and we pooled the three samples into one 6 mL sample per core and put in a 50 mL centrifuge tube covered in aluminum foil to avoid light penetration. The samples were immediately frozen (-20 ºC) until subsequent extraction and analysis. After thawing at 4 ºC overnight, we drew a subsample of 2 mL sediment from each sample, weighed and dried it at 60 ºC for 72 hours to obtain wet weight (g) dry weight (g), DBD and water content (%). We extracted the chlorophyll using ethanol (99.5 %) and, after diluting and incubating overnight, measured fluorescence using a Turner TD-700 fluorometer (Turner Designs). We calculated chlorophyll *a* content (g m^{-2}) using a modified equation from Hannides et al. (2014).

2.4 Data analyses

2.4.1 Flux calculations

We calculated oxygen fluxes in the benthic chambers (BC) as the difference in solute concentration between the onset and termination of each incubation as

$$F_{O2}\ (\text{mmol}\ O_2\ m^{-2}h^{-1}) = \frac{\Delta O_2}{\Delta t}\rho h \quad (1)$$

where ΔO_2 is the change in O_2 concentration in mmol kg^{-1} between start and end of incubation, *dt* is the duration of the incubation in hours, ρ is the density of the seawater in kg m^{-3} and *h* is the height of the chambers from the top to the sediment surface in meters. We calculated the flux of salinity-normalized TA ($nTA = TA/S_{in\ situ} \times S_{mean}$) in the same way:

https://doi.org/10.5194/bg-2023-173
Preprint. Discussion started: 4 October 2023

$$F_{TA}\ (\text{mmol TA}\ m^{-2}h^{-1}) = \frac{\Delta nTA}{\Delta t}\rho h \quad (2)$$

Similarly, we used DIC measurements to obtain fluxes as

$$F_{DIC}\ (\text{mmol C}\ m^{-2}h^{-1}) = \frac{\Delta nDIC}{\Delta t}\rho h - 0.5F_{TA} \quad (3)$$

where $\Delta nDIC$ is the change in salinity-normalized DIC in mmol kg^{-1}. The subtraction of $0.5F_{TA}$ is to account for the effect of inorganic processes (i.e. calcification/$CaCO_3$ dissolution) on DIC according to the assumptions that net community calcification affects TA and DIC in a ratio of 2:1 and NCP only modifies DIC (Smith and Key, 1975). F_{DIC} thus represents the DIC flux stemming from primary production and respiration only.

We calculated the photosynthetic (PQ) and respiratory (RQ) quotients from absolute fluxes in transparent and dark chambers, respectively, as

$$PQ = \frac{|F_{O2,light} - F_{O2,dark}|}{|F_{DIC,light} - F_{DIC,dark}|} \quad (4)$$

and

$$RQ = \frac{|F_{DIC,dark}|}{|F_{O2,dark}|} \quad (5)$$

Due to issues with the dark incubations in the natural meadow, RQ from this site was instead calculated as the average of the three other sites.

We computed EC fluxes from the high frequency time series following a multiple-step protocol described in Attard et al. (2019). In short, we bin-averaged the time series to 8 Hz, extracted fluxes for consecutive 15 min time windows using linear detrending (Mcginnis et al., 2014) and corrected fluxes for oxygen storage within the canopy (Rheuban et al., 2014b). Subsequently, we bin-averaged 15 min fluxes to 1 hr for interpretation. We defined F_{light} and F_{dark} based on when incident PAR was above or below 1 µmol m^{-2} s^{-1}, respectively. All sites experienced 19 light hours and 5 dark hours on average. We calculated daily metabolic parameters gross primary productivity (GPP) as

$$GPP\ (\text{mmol}\ m^{-2}d^{-1}) = \left(F_{light} + |F_{dark}|\right) \times t_{day} \quad (6)$$

where t_{day} is the number light hours. We calculated community respiration (CR) as

$$CR(\text{mmol}\ m^{-2}d^{-1}) = F_{dark} \times 24 \quad (7)$$

and net community productivity (NCP) as

$$NCP\ (\text{mmol}\ m^{-2}d^{-1}) = GPP - |CR| \quad (8)$$

We converted oxygen-based daily metabolic fluxes to DIC fluxes by multiplying F_{light} and F_{dark} with our empirically derived PQ and RQ, respectively:

$$F_{light\_DIC}\ (\text{mmol DIC}\ m^{-2}h^{-1}) = F_{light} \times \frac{1}{\overline{PQ}} \quad (9)$$

$$F_{dark\_DIC}\ (\text{mmol DIC}\ m^{-2}h^{-1}) = F_{dark} \times -\overline{RQ} \quad (10)$$

We then recalculated daily metabolic DIC fluxes GPP_{DIC}, CR_{DIC} and NCP_{DIC} (mmol DIC m^{-2} d^{-1}) using Eq. (6) – (8). Due to lack of information on the temporal variability in PQ and RQ, we only interpret DIC fluxes on a daily basis.

https://doi.org/10.5194/bg-2023-173
Preprint. Discussion started: 4 October 2023

277 **2.4.2 Biodiversity**

278 We evaluated biodiversity both from a taxonomic and a functional perspective. For taxonomic diversity, we used
279 the *vegan* package in R (Oksanen et al., 2019) to compute Shannon diversity (H') and Pielou's evenness
280 component (J'). H' was converted to effective numbers (H_{eff} =exp(H')) to make it linear and scale to species
281 richness (Jost, 2006). For functional diversity, we first assigned functional traits to each species based on existing
282 literature (Österling and Pihl, 2001; Queirós et al., 2013; Törnroos and Bonsdorff, 2012; Remy et al., 2021;
283 Kindeberg et al., 2022; Riera et al., 2020) and the databases Biological Traits Information Catalogue (Marlin,
284 2023) and Polytraits (Faulwetter et al., 2014). We then constructed a traits-by-species matrix assigning each
285 species to trait categories (Table S3). To avoid a disproportionally large influence by generalist species on
286 functional diversity, we used fuzzy coding (Chevenet et al., 1994) whereby species comprising multiple trait
287 categories were assigned a score between 0 and 3, with the total sum of each trait always being 3. Based on this
288 matrix, we calculated community-weighted means of trait values (CWM) and several multivariate components of
289 functional diversity including functional richness (FRic), functional evenness (FEve) and Rao's quadratic entropy
290 (RaoQ). These calculations were performed using the *FD* package in R (Laliberté and Legendre, 2010) and further
291 detailed information on these multivariate components and their taxonomic analogs can be found in Mason et al.
292 (2005) and Villéger et al. (2008). As with H', the functional diversity index RaoQ was transformed to effective
293 numbers as FD_{eff} = 1/(1-RaoQ).

294 We measured biomass divided into classes. We obtained wet weight (g) after blotting each specimen on
295 a tissue for two seconds and dry weight (g) after drying at 60 °C for 24 hours. Regrettably, due to a computer
296 malfunction the class division per sample was lost for infauna samples and only total, pooled biomass per site is
297 available for this group. We combusted pooled samples at 520 °C for 4 hours to obtain ash-free dry weight
298 (AFDW, g m^{-2}).

299 **2.4.3 Light-use efficiency**

300 We evaluated the relationship between irradiance (PAR) and gross primary productivity (GPP) using a hyperbolic
301 tangent function (Jassby and Platt, 1976; Platt et al., 1980):

$$GPP = P_m \times \tanh\left(\frac{\alpha PAR}{P_m}\right) \quad (11)$$

302 where P_m is maximum oxygen flux of gross primary productivity (mmol O_2 m^{-2} h^{-1}), α is the quasi-linear initial
303 slope of the curve and PAR is seabed irradiance as photosynthetic active radiation (µmol photons m^{-2} s^{-1}). We
304 performed curve-fitting in OriginPro 2022 using a Levenberg–Marquardt iteration algorithm, and we scaled the
305 standard error of the fitting parameters with the square root of the reduced chi squared statistic (Attard & Glud
306 2020).

307 To examine these relationships further, we calculated the light-use efficiency (LUE) at each site, which
308 indicates the efficiency with which absorbed PAR is converted to primary production, as:

$$LUE = \frac{GPP}{PAR \times fAPAR} \quad (12)$$

309 where fAPAR is the fraction of absorbed irradiance calculated from the difference between incident and reflected
310 PAR as measured by the upward and downward facing PAR sensors (see above). Including fAPAR in the
311 calculation of LUE thereby accounts for any differences owing to meadow characteristics such as the higher three-

https://doi.org/10.5194/bg-2023-173
Preprint. Discussion started: 4 October 2023

dimensional meadow complexity (higher fAPAR) relative to bare sediment (lower fAPAR) and captures the diel differences in seabed reflectance and absorption (Attard and Glud, 2020).

2.4.4 Statistical models

To test the effect of differences in abiotic factors between deployments, and thereby validate the use of the chronosequence approach, we employed linear mixed-effects models (package *lme4* in R (Bates et al., 2015), testing the effect and interaction of abiotic variables on absolute values of oxygen fluxes ($|F_{O2}|$). We used model selection (based on Akaike information criterion, AIC) to select the best model, which included sea surface temperature, flow velocity and PAR as fixed effects and site as a random factor. We used type III ANOVA for significance testing of fixed effects and likelihood-ratio tests (LRT) for the random effect. Assumptions of models were tested using the *performance* package in R (Lüdecke et al., 2020). oxygen fluxes calculated by the EC and BC using a two-sample t-test and compared oxygen and DIC fluxes in the benthic chambers using linear regression analyses. We tested site differences in biodiversity and sediment parameters using multiple one-way ANOVAs and visually reviewed multivariate community composition using non-metric multidimensional scaling (NMDS) and principal components analyses (PCA). We set significance level to α=0.05 for all statistical tests and performed all analyses in R, version 4.2.3 (Rcoreteam, 2023).

2.4.5 Carbon budget

We constructed a carbon budget of daily inorganic carbon fluxes and pools of organic carbon. We based the sediment carbon pool on the POC stock of the top 12 cm of sediment whereas we inferred seagrass aboveground and belowground carbon from dry weight (DW) and a global average carbon content for *Z. marina* of 34 % DW (Duarte, 1990). We estimated macroalgal carbon content based on DW and species-specific carbon content of the dominant red and brown algae reported from the area, which ranged from 29.1–39.9 % DW (Olsson et al., 2020). For benthic fauna, we converted ash-free dry weight (AFDW) to carbon, assuming a 50 % carbon content (Wijsman et al., 1999; Rodil et al., 2021). We converted organic carbon pools to moles and they are reported as mol C m^{-2}. Lastly, we calculated the total pool of organic carbon for each site as the sum of all pool means. We calculated the total propagated uncertainty (SE_{total}) as:

$$\boldsymbol{SE_{total}} = \sqrt{\sigma^2_{sediment} + \sigma^2_{AG} + \sigma^2_{BG}} + \sigma^2_{algae} + \sigma^2_{fauna} \Big/ \sqrt{\boldsymbol{n}} \quad (13)$$

where σ is the standard deviation of each pool mean and n is the number of pools. AG and BG is eelgrass aboveground and belowground biomass, respectively.

https://doi.org/10.5194/bg-2023-173
Preprint. Discussion started: 4 October 2023

340 **3. Results**

341 **3.1 Environmental conditions**

342 The weather was sunny and dry during all field deployments with only two minor rain events in between (Fig.
343 S1). Sea surface temperature ranged from 17.10–19.98 ºC, driven mainly by the diel light cycle. Salinity ranged
344 from 24.7 to 28.9 but remained constant (±0.1) during each individual deployment. Photosynthetic active radiation
345 (PAR) at the seabed was similar between sites and deployments and reached a highest value of 728 µmol m^{-2} s^{-1}
346 (Fig. 2; Fig. S1). Flow velocities ranged from 0.9 to 21 cm s^{-1}, averaging 5.6±3.4 cm s^{-1} across all sites (Fig. 2;
347 Fig. S1).

348 Ambient seawater chemistry was largely similar between sites, although there was a higher background
349 salinity, TA, DIC and DIN at the 3 yr and Nat site, which were sampled after a weather front passed by likely
350 exchanging some of the bay water with off-shore fjord water (Table S1; Fig. S1). Average DO during deployments
351 was highest in Bare and lowest in 3 yr, averaging (mean±sd) 302.9±21.8 and 260±37.3 µM, respectively.

352 **3.2 Hourly oxygen fluxes**

353 Hourly O_2 fluxes followed the diel light cycle and increased both in magnitude and variability going from bare
354 sediments to increasing age of the restored seagrass (Fig. 2).

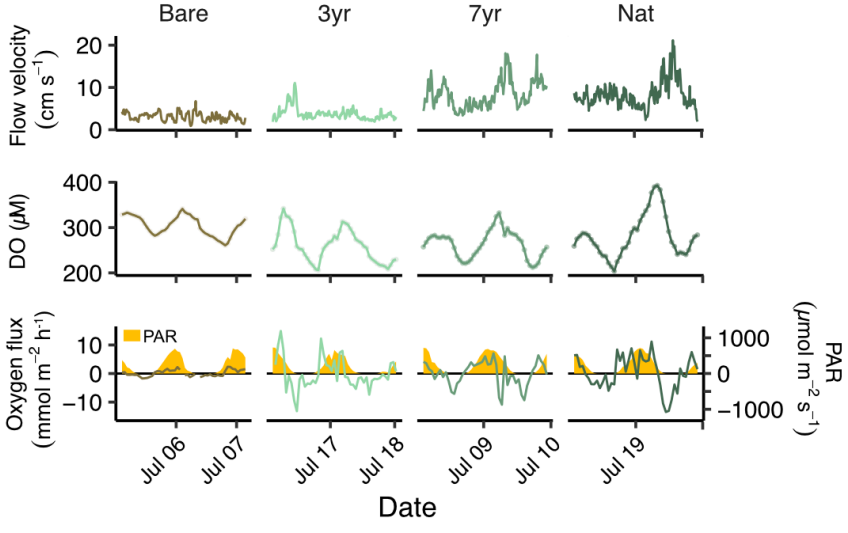

355

356 **Figure 2 Time series of flow, oxygen and light. Time series of (a) flow velocity, (b) ambient dissolved oxygen and (c)**
357 **hourly oxygen flux overlaid on photosynthetic active radiation (PAR) in yellow.**

358 The largest hourly oxygen fluxes typically occurred in the afternoon, with highest recorded between 14:30–15:30
359 in the 3 yr site (8.96±1.44 mmol m^{-2} hr^{-1}). The largest oxygen uptake rates were generally observed during hours
360 following midnight, with the most negative hourly flux recorded between 23:30–00:30 in Nat (-9.08±5.62 mmol
361 m^{-2} hr^{-1}).

362 Flow velocity was on average significantly higher in the 3 yr compared to Bare and significantly higher
363 in the 7 yr and Nat meadow compared to the 3 yr (Tukey HSD: $p<0.05$). Although there was a general positive
364 linear relationship between flow velocity and absolute oxygen flux across all deployments, the higher flow

https://doi.org/10.5194/bg-2023-173
Preprint. Discussion started: 4 October 2023

365 velocities in 7 yr and Nat generally occurred during short time periods at night and did not correspond to consistent
366 increases in absolute oxygen fluxes for those sites (Fig. S2). Further analysis through linear mixed effects
367 modelling indicated that while PAR and flow velocity explained a large portion of the variation in hourly $|F_{O2}|$,
368 the random effect Site was highly significant (LRT = 14.7, $p < 0.001$) suggesting that some other feature, not
369 included in the model, contributed to the observed differences in oxygen fluxes between sites.

370 **3.3 Daily integrated metabolism**

371 Daily metabolic oxygen fluxes (GPP, CR) as measured by the EC were lowest in the bare sediments and increased
372 with meadow age (Fig. 3a). GPP and CR were tightly coupled but |CR| was always higher than GPP, amounting
373 to an average GPP:CR ratio of 0.81 (Fig. 3b). Accordingly, we observed net heterotrophy at all sites (NCP < 0;

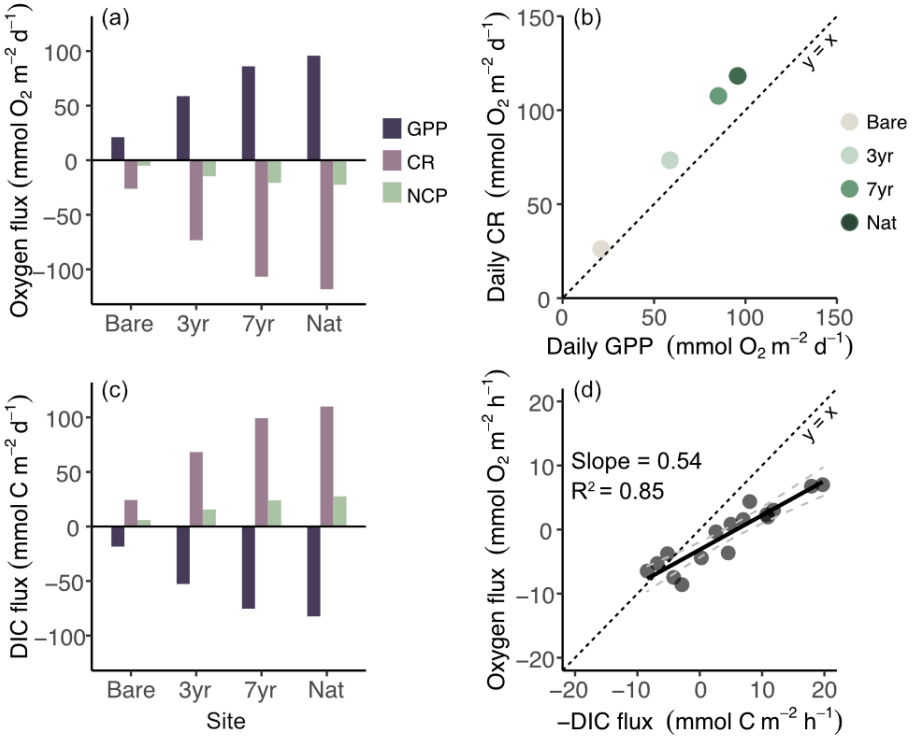

Figure 3 Fluxes and relationships of oxygen, carbon and productivity dynamics. a) Daily oxygen fluxes of gross primary productivity (GPP), community respiration (CR) and net community productivity (NCP). b) Linear regression of daily oxygen-based GPP and CR; c) Daily dissolved inorganic carbon (DIC) fluxes based on eddy covariance fluxes converted using photosynthetic (PQ) and respiratory (RQ) quotients d) Linear regression between of oxygen and dissolved inorganic carbon (DIC) hourly flux measured in the benthic chambers used to calculate PQ and RQ. Dashed black line indicates slope=1 and dashed grey lines are 95 % confidence interval of the fitted slope.

374 Fig. 3a–b). NCP increased three-fold between the bare and the youngest restored meadow (-5 to -15 mmol m^{-2} d^{-1})
375 with a further 40 percent increase in the seven-year-old meadow (21 mmol m^{-2} d^{-1}).

376 Oxygen fluxes measured by the EC and BC were not significantly different from each other (two-sample
377 t test: $p = 0.69$), although there was a tendency to overestimate oxygen fluxes in BC relative to EC by 0.7–4.0
378 mmol m^{-2} hr^{-1}. Oxygen and DIC fluxes in the benthic chambers were highly correlated across all incubations (Fig.
379 3d), irrespective of differences in light conditions. The photosynthetic quotient (PQ) was always less than unity,

https://doi.org/10.5194/bg-2023-173
Preprint. Discussion started: 4 October 2023

averaging 0.46±0.10 across the four sites, whereas the respiratory quotient (RQ) averaged 0.93±0.25. Site-specific RQ revealed high variability within and between sites ranging from 0.65–1.13.

Estimated DIC fluxes mirrored those of O_2 and the benthic DIC net efflux (NCP_{DIC}) increased as a function of meadow age from 6 mmol m^{-2} d^{-1} in the bare sediments to 28 mmol m^{-2} d^{-1} in the natural meadow, thus confirming the net heterotrophic status of the meadows as determined using oxygen fluxes (Fig. 3b, 3c).

3.4 Structural and functional diversity

3.4.1 Meadow properties

All three eelgrass sites were characterized by high spatial heterogeneity within each meadow (Table 1). We did not observe any significant differences in seagrass morphometry such as shoot density, canopy height or biomass. The only seagrass parameter that differed between the meadows was the number of reproductive shoots containing seeds that were significantly higher in the natural meadow ($p = 0.004$). However, the abundance and biomass of other macrophyte species such as brown and red macroalgae increased markedly with meadow age. In the 3 yr meadow, only a small specimen of the brown algae *Spermatochnus paradoxus* was found in one sample whereas in the natural meadow large quantities of up to five different macroalgal species were found. However, due to large variability in biomass between samples within each site (Table 1), the between-site differences in number of species were not statistically significant (ANOVA, $p>0.05$). The composition of macrophyte species became more even with meadow age such that while the 3 yr meadow was dominated by *Z. marina* (~99 % of total macrophyte biomass), the 7 yr and the natural meadow had a more heterogenous and evenly distributed macrophyte community, where *Z. marina* on average contributed 90±15 % and 64±32 %, respectively, to total macrophyte biomass (Table 1). As a result, the three-dimensional complexity of the canopy increased with meadow age, driven mainly by large-bodied drifting fucoid species (*F. serratus* and *F. vesiculosus*) and red algae *Furcellaria lumbricalis* residing, unattached, within the canopies.

Benthic microalgae, as inferred from chlorophyll *a* on the sediment surface, showed the opposite trend and decreased with meadow age and chlorophyll *a* was significantly lower in sediments underlying 7 yr (0.28±0.03 g m^{-2}) and Nat (0.26±0.01 g m^{-2}) compared to Bare (0.56±0.07 g m^{-2}).

Table 1 Eelgrass and macroalgal structural diversity. Morphometrics, biomass and diversity of the sites (mean±SE). 'Rep. shoots' represents reproductive shoots with seed spathes present. AG and BG are aboveground and belowground eelgrass biomass, respectively, as captured by sediment cores. Macroalgal biomass represents macroalgae collected in eelgrass canopy samples and maximum number of species refers to the number of macroalgal species found in a sample. Relative proportion is the macroalgal biomass relative to total macrophyte biomass. Species richness, diversity (H_{eff}) and evenness (J') refer to macrophytes including macroalgae and eelgrass.

Parameter	Unit	3 yr	7 yr	Nat
		Eelgrass		
Shoot density	m^{-2}	153±21	153±14	151±21
Shoot length	cm	43.3±2.1	39.0±0.2	40.0±1.2
Rep. shoots	m^{-2}	9±5	3±3	32±3
AG biomass	g m^{-2}	190.4±38.4	121.4±17.7	151.6±52.0
AG core	g m^{-2}	117.3±77.8	132.5±67.0	108.9±49.2
BG core	g m^{-2}	126.4±63.3	259.6±54.7	104.3±59.4
AG:BG	-	2.6±1.6	0.5±0.2	0.8±0.2
		Macroalgae		
Macroalgal biomass	g m^{-2}	0.004±0.004	16.3±15.4	131.6±94.3
Max no. of species	-	1	2	4
		Macrophyte diversity		

https://doi.org/10.5194/bg-2023-173
Preprint. Discussion started: 4 October 2023

Relative proportion	%	0.002±0.002	9.4±8.7	35.6±18.4
Species richness		1.3±0.3	3±0	3.3±1.5
Diversity (H_{eff})	-	1.0±0.0	1.3±0.3	2.1±0.6
Evenness (J')	-	0.001±0.0	0.2±0.2	0.7±0.0

411

412 **3.4.2 Benthic fauna**

413 We collected a total of 1927 individuals belonging to 43 taxa. Taxonomic diversity parameters (abundance,
414 number of species, Shannon diversity, evenness) exhibited large within-site variability illustrating the small scale
415 (<10 m) heterogeneity of fauna community structure. These parameters were always higher in vegetated relative
416 to bare sediments but exhibited variable, but generally non-significant, differences between the eelgrass sites (Fig.
417 4; Table S2). Abundance of infauna was highest in the 3 yr site, dominated by opportunistic polychaetes (e.g.
418 *Capitella capitata*). Yet, the high abundance in the 3 yr site did not result in a corresponding spike in total infaunal
419 biomass but was reflected by the lowest evenness of all sites (J'=0.47±0.08). In the 7 yr, abundance had decreased
420 by a third while species diversity (H_{eff}) and evenness (J') nearly doubled, exhibiting similar values as the natural
421 reference meadow (Table S2). Functional trait metrics revealed that both the functional group richness (FGR) and
422 functional diversity (FD_{eff}) was significantly higher in 7 yr and Nat compared to 3 yr and Bare which exhibited
423 similar values (Table S2). Functional richness (FRic) was low in the bare sediments (0.06±0.05) and tended to
424 increase with meadow age obtaining highest mean value in the natural meadow (0.53±0.11) but due to high within-
425 site variability, FRic was not statistically different between sites (Fig. 4c).

426 When separately targeting the meadows for epifauna, we found that they were species rich and highly
427 diverse, ranging from 15–18 species and H_{eff} from 7.4–10.9. However, neither taxonomic nor functional diversity
428 metrics exhibited any significant differences between the meadows, although there were some increasing trends
429 in especially functional evenness (FEve) which was highest in Nat and lowest in 3 yr (Table S2). Epifaunal
430 biomass increased on average three-fold in Nat compared to the two restored meadows and also had the highest
431 within-site variability (15.89±10.48 g m^{-2}) driven mainly by gastropods.

432 Community composition partly shifted as the meadow grew whereby bare sediments and the youngest
433 restored meadow were dominated by polychaetes whereas more epifaunal species such as bivalves and
434 crustaceans increased in older meadows (Fig. 4d). Absolute abundances and biomass supported this, of which
435 also bryozoans and gastropods contributed to higher biomass in Nat relative to Bare. However, multivariate
436 visualization of the different communities indicated that there was much overlap in community composition (Fig.
437 S3).

438 Based on our functional traits analyses, certain bioturbation modes became more prevalent as a function
439 of meadow age (Table S3). For instance, community-weighted means (CWM) of biodiffusors increased linearly
440 with meadow age and was significantly higher in the natural meadow and 7 yr compared to the 3 yr ($F_{3,20} = 8.4$;
441 $p < 0.001$). Surficial modifiers among infauna were higher in eelgrass compared to bare sediment and peaked in
442 the oldest restored meadow at a CWM of 0.29±0.10.

https://doi.org/10.5194/bg-2023-173
Preprint. Discussion started: 4 October 2023

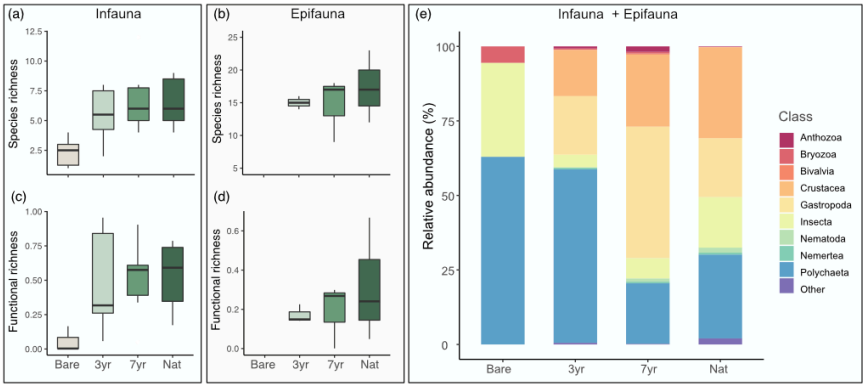

Figure 4 Biodiversity patterns in benthic fauna. Panels to the left show species richness (a–b) and functional richness (c–d) of infauna samples (a & c) and epifauna samples (b & d). Large panel to the right (e) shows relative abundance of different classes of all fauna combined (infauna + epifauna).

3.5 Sediment carbon stocks

The sediment within Gåsö bay eelgrass meadows has previously been reported as silty sand, with a median grain size (D_{50}) of the surface sediment between 140–170 µm and a silt-clay content of 26-35% (Infantes et al., 2022; Dr. Martin Dahl, pers. comm.). Concentrations of sediment OM, POC and TN were not significantly different between sites ($p < 0.05$) and did not display any consistent increases or decreases with meadow age (Table 2). However, when integrating the POC density across the top 12 cm, the highest POC stock was found in a natural meadow core (1529 g m^{-2}) and the lowest in a bare sediment core (209 g m^{-2}). Yet, due to large within-site variability, the sites were not significantly different from each other ($F_{3,8}$=1.52; p=0.28; Table 2). The lack of a clear trend with meadow age was further demonstrated by the 3 yr site, which had, on average, 32 % larger carbon stock than the 7 yr, and the 7 yr site was in turn more similar to the bare sediments site (Table 2). Depth profiles of POC concentration and density down to 20 cm revealed near-constant values down to between 12–16 cm where it started to increase (Fig. S4). Natural eelgrass had the highest average POC profile, but average values were highly skewed by one core replicate displaying POC density four times as high as the other two replicates in the site.

Table 2 Sediment properties across sites. Organic matter (OM), particulate organic carbon (POC), particulate inorganic carbon (PIC), total nitrogen (TN) and dry bulk density (DBD) of the top 2 cm of sediment. POC stock is the depth-integrated carbon stock over 0–12 cm sediment depth. Values are mean±SE, n=3 per site.

Site	OM (%)	POC (%)	PIC (%)	TN (%)	DBD (g cm^{-3})	POC_{stock} (g m^{-2})
Bare	3.80±0.23	0.88±0.14	0.55±0.06	0.25±0.02	0.37±0.08	343±93
3 yr	5.42±0.56	1.76±0.26	0.18±0.04	0.34±0.03	0.37±0.07	652±142
7 yr	5.36±0.34	1.54±0.31	0.61±0.21	0.34±0.01	0.24±0.03	494±39
Nat	4.98±0.78	1.11±0.11	0.64±0.30	0.29±0.04	0.34±0.06	883±332

https://doi.org/10.5194/bg-2023-173
Preprint. Discussion started: 4 October 2023

3.6 Light-use efficiency

All meadows experienced similar incident light conditions (Fig. 5a). The fraction of absorbed light (*f*APAR) was always higher in eelgrass (~97 %) compared to bare sediments (~94 %) but did not differ between eelgrass sites on a daily basis (Fig. 5b). Hourly GPP tracked PAR with a clear hysteresis effect evident in the 7 yr and natural meadow but to a lesser extent in the bare site (Fig. 5c; Fig. S5). P-I relationships were best explained by the hyperbolic tangent function yielding R^2 between 0.45–0.74. The irradiance needed for photosynthesis to balance respiration (I_k) was almost four times higher in the bare site compared to the 7 yr site, equaling 380 and 97 µmol photons m^{-2} s^{-1}, respectively (Table S4; Fig. 5d). Estimated light-use efficiency (LUE) was lowest in Bare (0.001 O_2 photon^{-1}) and increased with meadow age to 0.004 and 0.005 O_2 photon^{-1} in 3 yr and 7 yr, respectively. The highest daily LUE was observed in Nat (0.007 O_2 photon^{-1}) coincident with the highest number of macrophyte species and the most diverse community structure.

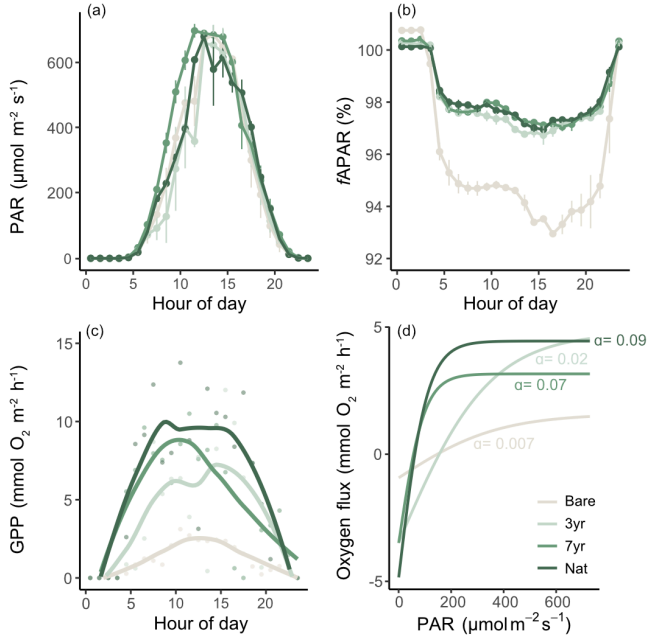

Figure 5 Light-use efficiency and productivity relationships. Panels a–c show different components of light-use efficiency (LUE) as a function of hour of the day: a) incident photosynthetic active radiation (PAR); b) fraction of absorbed PAR (fAPAR); c) shows gross primary productivity (GPP) as a function of time of day and; d) shows the relationship between oxygen flux and PAR as hyperbolic tangent curves estimated for each site.

Similar to LUE, GPP and |CR| displayed a positive linear relationship with number of macrophyte species. There was also a positive trend between these parameters and macrophyte Shannon diversity (H_{eff}) and the proportion of macroalgal biomass relative to eelgrass biomass, respectively (Fig. 6).

Table 3 Daily metabolism as a function of meadow age. Curve fitting of daily metabolism parameters GPP, CR and NCP to meadow age (SiteAge) converted to logarithmic scale ($log_{10}(x+1)$). SiteAge for the site Bare was defined as 0 and 13 years for the natural meadow.

Metabolic parameter	Function	p	R^2
GPP	$GPP = 67.29 \pm 4.63 \times \log_{10}(\text{SiteAge} + 1) - 20.80 \pm 3.65$	0.005	0.99

https://doi.org/10.5194/bg-2023-173
Preprint. Discussion started: 4 October 2023

CR	$CR = -83.08 \pm 5.77 \times \log_{10}(\text{SiteAge} + 1) - 26.06 \pm 4.56$	0.005	0.99
NCP	$NCP = -15.79 \pm 1.26 \times \log_{10}(\text{SiteAge} + 1) - 5.26 \pm 0.99$	0.006	0.98

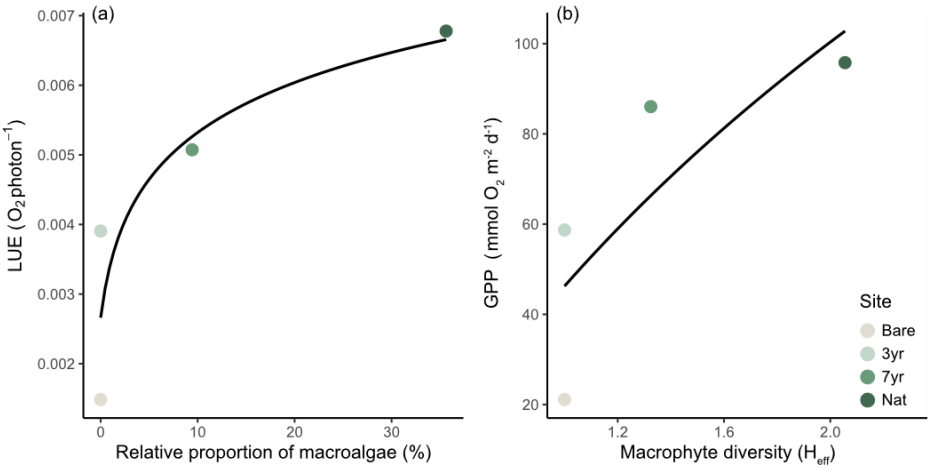

Figure 6 Biodiversity and productivity relationship. (a) Light-use efficiency (LUE) as a function of the relative biomass of macroalgae to eelgrass ($R2_{adj}$= 0.70). (b) Gross primary productivity (GPP) as a function of macrophyte Shannon diversity index ($R2_{adj}$= 0.46); Black lines represent best fit ($\log_e(x+1)$). Note that the bare site was not quantitatively sampled for macroalgal proportions or macrophyte diversity and was a posteriori set to 0 % in and 1, respectively, for curve fitting.

3.7 Carbon pools

Converting seagrass community components to carbon illustrates the pools of carbon available for export, remineralization or burial. Notably, total carbon pools were higher in eelgrass relative to bare sediment but were similar between restored and natural seagrass (Table 4). Sediment POC stocks were the largest carbon pools followed by eelgrass biomass which contributed on average 11, 21 and 7 percent to the total carbon pool in the 3 yr, 7 yr and natural meadow, respectively (Table 4).

Table 4. Carbon pools. Pools of particulate organic carbon (mean±SE, mol m^{-2}) in the different components of the benthic habitats. AG and BG are above- and belowground eelgrass biomass, respectively. Fauna is total fauna (infauna+epifauna).

Site	Sediment	Eelgrass AG	Eelgrass BG	Macroalgae	Fauna	Total pool
Bare	28.54±7.71	0	0	n.d.	0.03	28.57±13.35
3yr	54.28±11.83	3.32±2.20	3.58±1.79	0.00±0.00	0.24	61.42±10.82
7yr	41.15±3.27	3.75±1.90	7.35±1.55	0.45±0.42	0.29	52.99±4.14
Nat	73.53±27.65	3.08±1.39	2.95±0.69	3.78±2.76	0.56	83.91±24.14

https://doi.org/10.5194/bg-2023-173
Preprint. Discussion started: 4 October 2023

4. Discussion

We present a comprehensive dataset of post-restoration seagrass development that captures several different components of seagrass metabolism. This enables investigating the role of biodiversity and different components of a seagrass ecosystem in carbon cycling. We show that i) community-integrated photosynthetic (GPP) and respiratory (CR) fluxes increase as a function of meadow age (Fig. 3); ii) daily |CR| increased more relative to GPP resulting in net heterotrophy (NCP<0) on diel timescales during summer; iii) diversity and biomass of macrophytes other than the restored seagrass could be driving higher primary productivity through increased light-use efficiency (Fig. 5); iv) faunal communities recover rapidly and attain species- and functional richness comparable to natural meadows within seven years since restoration (Fig. 4); v) surficial (0–12 cm) sediment carbon stocks are large but are not significantly affected by the presence of seagrass in this sheltered bay.

Based on the above results, we postulate that while higher diversity of macrophytes contribute to elevated GPP and CR, the additional CR stemming from benthic fauna communities together with labile organic matter input push diverse seagrass meadows toward summer net heterotrophy. This illustrates potential tradeoffs between climate change mitigation and biodiversity conservation as incentives for seagrass restoration. Below we discuss four main lines of evidence to support this postulation.

4.1 Metabolic fluxes scale to meadow development

We found large daily fluxes of GPP- and CR derived O_2 and DIC that increased as the system developed from bare sediments to a mature meadow (Table 3; Fig. 3). Our values are relatively low when comparing to global average GPP, CR and NCP estimated for temperate seagrasses of 166±14, 130±11 and 34±8 mmol O_2 m^{-2} d^{-1}, respectively (Duarte et al., 2010). Yet, it should be noted that discrepancies owing to methodological differences are difficult to account for. An updated assessment of seagrass NCP in temperate areas reported an average of 29±79 mmol O_2 m^{-2} d^{-1}, although the study which covered 187 seagrass metabolism studies found that merely 68 % reported net autotrophy (Ward et al., 2022). Accordingly, the notion that seagrass habitats are strongly net autotrophic is being increasingly contested as methods continue to improve. In all our sampled sites, GPP was lower than |CR| resulting in net heterotrophy (negative NCP), independently established both by EC oxygen fluxes and benthic chamber DIC and oxygen fluxes. Several recent studies have reported instances of sustained net heterotrophy across multiple seagrass species and environments (e.g. Barron et al., 2006; Rheuban et al., 2014a,b; van Dam et al., 2019; Berger et al., 2020; Attard et al., 2019; Berg et al., 2022, Ward et al., 2022). For instance, a recent study of *Z. marina* using EC reported GPP and CR values similar to our natural meadow (95 and 94 mmol O_2 m^{-2} d^{-1}, respectively) resulting in a near balanced metabolic state across 11 years of monitoring (Berger et al., 2020). The authors reported a generally balanced metabolic state on monthly timescales but following a temperature-driven dieback event that diminished seagrass shoot density, GPP and |CR| decreased by 55 % and 48 %, respectively. This shifted the meadow to net heterotrophy during summer (NCP = -26±15 mmol O_2 m^{-2} d^{-1}). In the following years, the gradual increase in seagrass shoot density increased primarily GPP, showing clear signs of seagrass recovery (Berger et al., 2020).

Although GPP often substantially increases during summer in temperate seagrass meadows, so does CR to a similar extent (Ward et al., 2022). Consequently, despite large seasonal variability in photosynthesis and respiration, the metabolic state is often relatively stable on an annual basis, granted there are no major ecosystem

https://doi.org/10.5194/bg-2023-173
Preprint. Discussion started: 4 October 2023

regime shifts. While interannual variability of NCP has been related to seagrass die-off and recovery episodes (Berger et al., 2020), seagrass phenology linked to abiotic factors such as temperature and light regimes typically dictates the metabolic state on intra-annual timescales (e.g. Champenois and Borges, 2012; Rheuban et al., 2014a, b). Here, we show that biotic components other than the seagrass itself can contribute to both the magnitude and variability in metabolic fluxes. Irrespective of traditional seagrass metrics such as seagrass shoot density and biomass, GPP and |CR| consistently increased with meadow age which in turn corresponded to increased autotrophic diversity and macroalgal biomass.

4.2 Carbon and oxygen balance

As part of this study, we present a methodological approach that estimates *in situ* DIC fluxes under natural hydrodynamic and light conditions. This is obtained by combining the advantages of aquatic eddy covariance with the ability to constrain the marine carbonate system and oxygen dynamics using benthic chambers. Concurrent deployment of these two methods have been utilized in previous coastal studies (Camillini et al., 2021; Long et al., 2019; Polsenaere et al., 2021), but only for comparing oxygen fluxes.

Assessing the *in situ* relationship between oxygen (F_{O2}) and DIC fluxes (F_{DIC}) can provide insights into biogeochemical processes and renders reliable estimates of photosynthetic (PQ) and respiratory quotients (RQ). All else equal, photosynthetic and respiratory quotients are governed by the C:N:P ratio of the fixed and respired organic matter present in the system (Champenois and Borges, 2021). However, considering the various sinks and sources of organic matter present in a seagrass meadow and the multitude of processes affecting F_{O2} and F_{DIC} differently, this is not very useful. Deviations from the theoretical 1:1 relationship between F_{O2} and F_{DIC} (Fig. 3d) are thus ubiquitous in the literature (e.g. Turk et al., 2015; Barron et al., 2006; Trentman et al., 2023). In fact, the slope we observed is identical to what Pinardi et al. (2009) observed in sediments vegetated with the freshwater macrophyte *Vallisnera spiralis* using sediment cores. Moreover, our relatively low PQ's (0.34–0.52) were similar to what Ribaudo et al. (2011) observed in *V. spiralis* (0.30–0.68) in microcosms. The authors attributed the low PQ to oxygen transport to roots and subsequent radial oxygen loss (ROL) which fuels aerobic respiration, a process well-documented in *Z. marina* as well (e.g. Borum et al., 2007; Jensen et al., 2005; Frederiksen and Glud, 2006; Jovanovic et al., 2015). Turk et al. (2015) observed PQs ranging from 0.5–2.6 in seagrass (*Thallasia testudinium*) and found a temporal component to the variability of PQ with lower values in the morning and higher in the evening (Turk et al., 2015). Similar to our study, Ouisse et al. (2014) obtained a PQ and RQ of 0.42±0.27 and 0.95±0.22, respectively, using *in situ* benthic chambers in dwarf eelgrass (*Z. noltii*) meadows across several seasons. The authors hypothesized that the low PQ could also be due to photorespiration in epiphytic algae on the seagrass leaves which can consume more than three moles of O_2 for every mole DIC used (Ouisse et al., 2014). We observed large quantities of epiphytic microalgae and biofilm on seagrass leaves across all our studied meadows, albeit only as qualitative observations (Kindeberg, T., *pers. obs.*). However, seagrass epiphytes are abundant in the area where it can exert detrimental effects on seagrass metabolic performance and positive effects on epifauna distribution (Brodersen et al., 2015; Gullström et al., 2012; Baden et al., 2010). Other biogeochemical processes such as production and consumption of highly oxidized photosynthates could be another explanation, but that is merely speculative at this stage and needs further research. It is important to note that inorganic

https://doi.org/10.5194/bg-2023-173
Preprint. Discussion started: 4 October 2023

processes (i.e. $CaCO_3$ production and dissolution), which can have a large influence on PQ and RQ (Champenois and Borges, 2021), are implicitly accounted for in our F_{DIC} by subtraction of the $0.5F_{TA}$ term in Eq. (3).

While we obtained an average RQ close to unity, it was based on a relatively small sample size compared to PQ due to issues with dark incubations especially in the natural meadow. It is possible that our acclimation (~30 mins) or incubation times (~3 hours) were too short for accurately capturing dark DIC fluxes, as seen in the temporal lag in DIC fluxes relative to O_2 fluxes in a study by Fenchel and Glud (2000) and a lag in O_2 consumption due to the primary producer cellular machinery (Tang and Kristensen, 2007). Nonetheless, without any ancillary data on other biogeochemical processes we cannot reconcile the sources of our observed PQ and RQ.

4.3 Macrophyte diversity driving light-use efficiency and higher metabolism

Despite the large research field on the relationship between biodiversity and primary productivity (Tilman et al., 2014), light-use efficiency (LUE) is largely understudied in benthic metabolism studies (Attard and Glud, 2020). Studies have hitherto focused mainly on smaller-scale LUE, such as microalgae in microbial mats and corals (Brodersen et al., 2014; Al-Najjar et al., 2010; Al-Najjar et al., 2012). We observed a positive relationship between macrophyte diversity and LUE when controlling for biomass, indicating that mixed meadows consisting of both seagrass and macroalgae utilize light resources more efficiently and are more productive compared to monospecific meadows. Importantly, the restored seagrass meadows became more mixed over time as drifting macroalgae inhabited the meadow. These unattached algae are a common feature in the area, often considered a nuisance that can prevent seagrass recovery (Moksnes et al., 2018). Here it seems they also improve overall LUE of the meadow and contributes to larger metabolic fluxes.

Whether higher LUE is driven by certain species remains unclear, but the change in canopy structure and increasing three-dimensional complexity can positively influence LUE (Binzer et al., 2006; Zimmerman, 2003). Niche complementarity is common in ecological systems (Hooper et al., 2005; Loreau and Hector, 2001) and it is reasonable to believe that with increased diversity of autotrophs, pigment complementarity can facilitate optimal resource-use, especially as brown and red macroalgae are known to have a range of photosynthetic pigments (Enríquez et al., 1994). Additionally, the mere presence of multiple growth morphologies may induce self-shading that further increases LUE (Tait et al., 2014). An increase in photosynthetic pathways (e.g. C3 and C4) with higher macrophyte diversity and differing affinity for forms of inorganic nutrients (e.g. NH_4^+ and NO_3^-) is also expected. Moreover, both *Z. marina* and fucoid species are known to utilize both CO_2 and HCO_3^- for photosynthesis (Binzer et al., 2006). However, the efficiency differs between species (e.g. Larsson and Axelsson, 1999; Invers et al., 2001) and considering the large spatiotemporal variability in pH and $[HCO_3^-]$ relative to $[CO_2]$ we observed, this could be another reason for the higher LUE at higher species diversity. Studies from macroalgal canopies have found similar relationships between macrophyte canopy complexity and LUE, attributed to niche complementarity where intact assemblages are more efficient and productive than the sum of its parts (Tait and Schiel, 2011; Tait et al., 2014). For instance, a study by Tait and Schiel (2011) using *ex situ* incubation chambers found that an intact assemblage of seven species had higher net photosynthesis than the sum of all individual species. The authors observed that different species played different roles at different irradiances. For instance, the fucoid species *Cystophora torulosa* was exceptionally efficient at photosynthesizing at high irradiance and did not show signs of photoinhibition even at PAR > 2000 µmol m^{-2} s^{-1} (Tait and Schiel, 2011). Tait et al. (2014) studied P-I

https://doi.org/10.5194/bg-2023-173
Preprint. Discussion started: 4 October 2023

relationships in macroalgal assemblages and found that when more sub-canopy species where included (up to four) respiration and photosynthesis increased, thus corroborating our observed trends. However, they found that production did not saturate at incident irradiance of 2000 µmol m^2 s^{-1} as opposed to less speciose assemblages (2 sub-canopy species) that reached light saturation of net primary production (NPP) already at about 600 µmol m^2 s^{-1} (Tait et al., 2014). This is somewhat contrary to what we found for GPP, where P-I curves saturated at lower irradiance with higher macrophyte diversity (Fig. 5d; Fig. S5). Albeit not specifically addressing canopy structure or diversity, Rheuban et al. (2014a) found that a younger, five-year-old, restored *Z. marina* meadow was light-saturated while an older, 11-year-old meadow did not show any signs of light saturation, and this was consistent across seasons.

Whereas it is rather intuitive that a diverse community of primary producers are better at photosynthesizing (i.e. higher GPP), the relationship is as strong with CR. This is likely explained by the tight coupling between GPP and CR stemming from respiration of labile photosynthates (Penhale and Smith, 1977). However, detritus of macroalgae such as *Fucus* spp. is also more labile than *Z. marina*, partly due to a lower C:N ratio and a more bioavailable polysaccharide composition (e.g. Kristensen, 1994; Thomson et al., 2020).

4.4 The role of benthic diversity in seagrass metabolism

The fact that most fauna diversity metrics were not significantly different between the natural meadow and the youngest (3 yr) meadow implies that benthic diversity recovers quickly. Similar findings have recently been reported from *Z. marina* restoration projects in Denmark (Steinfurth et al., 2022) and from the very same sites as in this study (Gagnon et al., 2023). In fact, Gagnon et al. (2023) found that both taxonomic and functional diversity recovered within 15 months after restoration but already after 3 months the abundance was similar to documented abundances in comparable seagrass meadows in the area. The authors partly attributed this to efficient larval dispersal from the adjacent natural meadow within the bay (Gagnon et al., 2023).

It is generally established that higher diversity yields higher productivity in seagrass meadows (Duffy et al., 2017), although the mechanisms behind the relationship are debated (Hooper et al., 2005; Gamfeldt et al., 2015). Based on our results, it seems that high macrophyte and macrofauna diversity positively influence GPP and CR, respectively, although the relationships with fauna are less clear. Aside from direct cellular respiration, many infauna species indirectly modify metabolic fluxes across the sediment-water interface through bioturbation and sediment reworking (Aller and Aller, 1998; Kristensen et al., 2012). A scrutiny of bioturbation and reworking modes revealed that especially biodiffusors and surficial modifiers increased with meadow age, despite highest total abundance of infauna in the youngest meadow (Table S2–S3). It is possible that these functional modes benefited from larger quantities of macroalgal detritus building up on the sediment surface over the years. Thomson et al. (2020) found the lugworm *Arenicola marina*, an upward conveyor, contributed to a 37 % higher efflux of DIC in sediments containing *F. vesiculosus* compared to *Z. marina*. Macroalgal detritus was to a much higher extent respired or consumed compared to seagrass, which instead was buried in anoxic sediment layers by the lugworm (Thomson et al., 2020). Moreover, the role of bioturbation in oxygenating otherwise anoxic sediment can have large ramifications for sediment-water fluxes of DIC and could hence contribute to our observed CR.

https://doi.org/10.5194/bg-2023-173
Preprint. Discussion started: 4 October 2023

4.5 Implications of seagrass restoration on the carbon budget

The observed net heterotrophy during the productive season implies the system relies on either historic production of autochthonous carbon or on trophic subsidies to sustain metabolism. Albeit only covering a brief period within the summer season, our results suggest that the seagrass in this area receives large amounts of allochthonous carbon that is partly turned over and released as DIC. A large influx and sedimentation of allochthonous carbon was shown in a recent study by Dahl et al. (2023) from the same bay. They reported relatively high carbon accumulation rates (0.91±0.06 mol m^{-2} yr^{-1}) of which 51 % of sediment carbon originated from eelgrass productivity and 38 % from macroalgae (Dahl et al., 2023). Assuming this rate is constant throughout the year (0.0025 mol m^{-2} d^{-1}), this accumulation rate is about an order of magnitude lower than our measured summer NCP_{DIC}, implying that the majority of imported carbon is rapidly remineralized or assimilated by secondary producers (Fig. 7).

Our estimated budget of all carbon pools illustrates that whereas sediment stocks are the dominant pools, organic carbon is built up in living biomass following restoration (Table 4; Fig 7). Eelgrass and macroalgal biomass in the natural meadow made up 58 and 27 % of all biomass, respectively, which is on the same order as the relative proportion of sediment POC sources found in Dahl et al. (2023). Accumulation of sediment carbon and production of living biomass can be decoupled on longer time scales although trophic subsidies (i.e. external inputs) may be required to sustain both (Huang et al., 2015; Cebrian et al., 1997; Duarte et al., 2010).

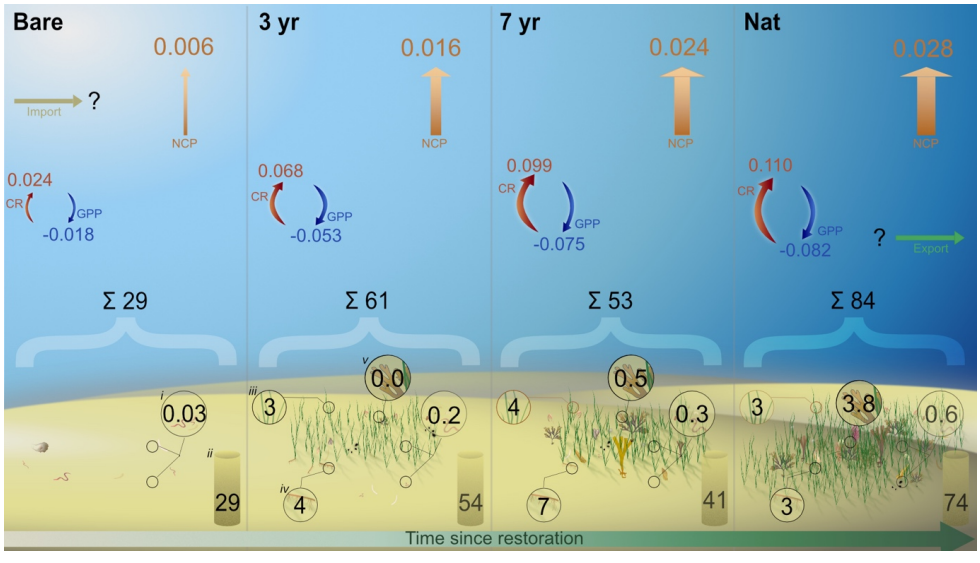

Figure 7 Pools and fluxes of carbon. Schematic illustration of a carbon budget including different benthic pools (mol C m^{-2}) of particulate organic carbon in i) fauna biomass, ii) sediment iii) eelgrass aboveground biomass, iv) eelgrass belowground biomass and v) macroalgal biomass. Arrows indicate the daily metabolic fluxes of dissolved inorganic carbon (mol m^{-2} d^{-1}) where blue arrows are gross primary productivity (GPP_{DIC}), red arrows are community respiration (CR_{DIC}) and orange arrows are net community productivity (NCP_{DIC}). Tan and green arrows indicate lateral import and export of particulate organic carbon, respectively.

While we are able to resolve the dominant carbon pools and metabolic fluxes, the import and export of organic carbon over seasonal timescales is required to reconcile the annual carbon cycling at this site. Nevertheless, it is

https://doi.org/10.5194/bg-2023-173
Preprint. Discussion started: 4 October 2023

683 reasonable to infer that NCP and carbon sequestration in these seagrass systems are sustained by lateral import of
684 allochthonous organic carbon.

685 **5. Conclusion**

686 Planting seagrass is a profound transformation of the benthic environment that influences biodiversity and carbon
687 cycling. In this field study, we found that while fauna diversity developed in an expected successional pattern, the
688 metabolic fluxes and net release of DIC were always higher in seagrass. These fluxes increased with meadow age
689 and we observed increasing gross primary productivity and respiration as the seagrass grew and drifting algae and
690 benthic fauna colonized. Collectively, our findings point to a plausible situation where higher macrophyte and
691 fauna diversity drives high primary productivity and respiration, respectively. Together with ample input of
692 sestonic organic matter to this sheltered bay, these productive meadows act as effective bioreactors of organic
693 carbon on diel timescales during summer, as evidenced by the net heterotrophic state and net efflux of DIC. These
694 results highlight relationships between carbon cycling and biodiversity that should be taken into consideration
695 when restoring seagrass, especially in sheltered environments with large input of external organic matter. Yet,
696 identifying the separate mechanisms and constraining the relative importance of fauna and flora diversity for
697 benthic carbon fluxes remains difficult and should be a focal point in future research.

https://doi.org/10.5194/bg-2023-173
Preprint. Discussion started: 4 October 2023

698 **Data availability**

699 The dataset is freely available in the Zenodo repository (https://doi.org/10.5281/zenodo.8363551).

700 **Author contributions**

701 TK conceived the study with input from KMA, CQ and EI. TK, KMA, CQ and EI designed the field study. TK,
702 KMA, JH, JM and EI conducted the field work. TK and KMA analyzed data. TK wrote the manuscript with input
703 from all co-authors. All authors approved the submitted version of the article.

704 **Conflict of interest statement**

705 The authors declare that the research was conducted in the absence of any financial or commercial relationships
706 that could be construed as potential conflicts of interest.

707 **Acknowledgements**

708 TK acknowledges funding from the Gyllenstiernska Krapperup Foundation (grant number KR2020-0066), the
709 European Union LIFE programme (grant number LIFE17 CCA/SE/000048) and the Royal Physiographic Society
710 of Lund (grant number 42518). KMA received funding from the Danish Institute for Advanced Study and CQ
711 received funding from SDU Climate Cluster. We thank Dr. Adam Ulfsbo for assistance with total alkalinity
712 analyses, Dr. Susanne Pihl Baden and Dr. Per Carlsson for help with fauna identification and Dr. Mirjam Victorin
713 for assistance with flux calculations. We are also grateful for the hospitality and assistance of the staff at
714 Kristineberg Center. Symbols used in figures courtesy of the Integration and Application Network, University of
715 Maryland Center for Environmental Science.
716

https://doi.org/10.5194/bg-2023-173
Preprint. Discussion started: 4 October 2023

References

Al-Najjar, M. A. A., de Beer, D., Kühl, M., and Polerecky, L.: Light utilization efficiency in photosynthetic microbial mats, Environmental Microbiology, 14, 982-992, https://doi.org/10.1111/j.1462-2920.2011.02676.x, 2012.

Al-Najjar, M. A. A., de Beer, D., Jørgensen, B. B., Kühl, M., and Polerecky, L.: Conversion and conservation of light energy in a photosynthetic microbial mat ecosystem, The ISME Journal, 4, 440-449, https://doi.org/10.1038/ismej.2009.121, 2010.

Aller, R. C. and Aller, J. Y.: The effect of biogenic irrigation intensity and solute exchange on diagenetic reaction rates in marine sediments, Journal of Marine Research, 56, 905-936, https://doi.org/10.1357/002224098321667413, 1998.

Attard, K. M. and Glud, R. N.: Technical note: Estimating light-use efficiency of benthic habitats using underwater O2 eddy covariance, Biogeosciences, 17, 4343-4353, https://doi.org/10.5194/bg-17-4343-2020, 2020.

Attard, K. M., Rodil, I. F., Glud, R. N., Berg, P., Norkko, J., and Norkko, A.: Seasonal ecosystem metabolism across shallow benthic habitats measured by aquatic eddy covariance, Limnology and Oceanography Letters, 4, 75-86, https://doi.org/10.1002/lol2.10107, 2019.

Baden, S., Boström, C., Tobiasson, S., Arponen, H., and Moksnes, P.-O.: Relative importance of trophic interactions and nutrient enrichment in seagrass ecosystems: A broad-scale field experiment in the Baltic− Skagerrak area, Limnology and Oceanography, 55, 1435-1448, https://doi.org/10.4319/lo.2010.55.3.1435, 2010.

Barron, C., Duarte, C. M., Frankignoulle, M., and Borges, A. V.: Organic carbon metabolism and carbonate dynamics in a Mediterranean seagrass (Posidonia oceanica) meadow, Estuaries Coasts, 29, 417-426, https://doi.org/10.1007/BF02784990, 2006.

Bates, D., Mächler, M., Bolker, B., and Walker, S.: Fitting Linear Mixed-Effects Models Using lme4, Journal of Statistical Software, 67, 1 - 48, https://doi.org/10.18637/jss.v067.i01, 2015.

Berg, P., Huettel, M., Glud, R. N., Reimers, C. E., and Attard, K. M.: Aquatic Eddy Covariance: The Method and Its Contributions to Defining Oxygen and Carbon Fluxes in Marine Environments, Annual Review of Marine Science, 14, 431-455, https://doi.org/10.1146/annurev-marine-042121-012329, 2022.

Berg, P., Delgard, M. L., Polsenaere, P., McGlathery, K. J., Doney, S. C., and Berger, A. C.: Dynamics of benthic metabolism, O2, and pCO2 in a temperate seagrass meadow, Limnology and Oceanography, 0, https://doi.org/10.1002/lno.11236, 2019.

Berg, P., Røy, H., Janssen, F., Meyer, V., Jørgensen, B. B., Huettel, M., and de Beer, D.: Oxygen uptake by aquatic sediments measured with a novel non-invasive eddy-correlation technique, Mar. Ecol.-Prog. Ser., 261, 75-83, http://dx.doi.org/10.3354/meps261075, 2003.

Binzer, T., Sand-Jensen, K., and Middelboe, A.-L.: Community photosynthesis of aquatic macrophytes, Limnology and Oceanography, 51, 2722-2733, https://doi.org/10.4319/lo.2006.51.6.2722, 2006.

Borum, J., Sand-Jensen, K., Binzer, T., Pedersen, O., and Greve, T. M.: Oxygen movement in seagrasses, in: Seagrasses: biology, ecology and conservation, edited by: Larkum, A. W. D., Orth, R. J., and Duarte, C. M., Springer, Dordrecht, 255-270, https://doi.org/10.1007/978-1-4020-2983-7, 2007.

Brodersen, K. E., Lichtenberg, M., Paz, L.-C., and Kühl, M.: Epiphyte-cover on seagrass (Zostera marina L.) leaves impedes plant performance and radial O2 loss from the below-ground tissue, Frontiers in Marine Science, 2, 58, https://doi.org/10.3389/fmars.2015.00058, 2015.

https://doi.org/10.5194/bg-2023-173
Preprint. Discussion started: 4 October 2023

764 Brodersen, K. E., Lichtenberg, M., Ralph, P. J., Kühl, M., and Wangpraseurt, D.: Radiative
765 energy budget reveals high photosynthetic efficiency in symbiont-bearing corals, Journal of
766 The Royal Society Interface, 11, 20130997, https://doi.org/10.1098/rsif.2013.0997, 2014.
767 Camillini, N., Attard, K. M., Eyre, B. D., and Glud, R. N.: Resolving community metabolism
768 of eelgrass Zostera marina meadows by benthic flume-chambers and eddy covariance in
769 dynamic coastal environments, Mar. Ecol.-Prog. Ser., 661, 97-114,
770 https://doi.org/10.3354/meps13616, 2021.
771 Cebrian, J., Duarte, C. M., Marbà, N., and Enriquez, S.: Magnitude and fate of the production
772 of four co-occurring western Mediterranean seagrass species, Mar. Ecol.-Prog. Ser., 155, 29-
773 44, https://doi.org/10.3354/meps155029, 1997.
774 Champenois, W. and Borges, A. V.: Seasonal and interannual variations of community
775 metabolism rates of a Posidonia oceanica seagrass meadow, Limnology and Oceanography,
776 57, 347-361, https://doi.org/10.4319/lo.2012.57.1.0347, 2012.
777 Champenois, W. and Borges, A. V.: Net community metabolism of a Posidonia oceanica
778 meadow, Limnology and Oceanography, 66, https://doi.org/10.1002/lno.11724, 2021.
779 Chevenet, F., Dolédec, S., and Chessel, D.: A fuzzy coding approach for the analysis of long-
780 term ecological data, Freshwater biology, 31, 295-309, https://doi.org/10.1111/j.1365-
781 2427.1994.tb01742.x, 1994.
782 Dahl, M., Asplund, M. E., Bergman, S., Björk, M., Braun, S., Löfgren, E., Martí, E., Masque,
783 P., Svensson, R., and Gullström, M.: First assessment of seagrass carbon accumulation rates in
784 Sweden: A field study from a fjord system at the Skagerrak coast, PLOS Climate, 2, e0000099,
785 https://doi.org/10.1371/journal.pclm.0000099, 2023.
786 Duarte, C. M.: Seagrass nutrient content, Mar. Ecol.-Prog. Ser., 201-207,
787 https://doi.org/10.3354/meps067201, 1990.
788 Duarte, C. M. and Cebrian, J.: The fate of marine autotrophic production, Limnology and
789 Oceanography, 41, 1758-1766, https://doi.org/10.4319/lo.1996.41.8.1758, 1996.
790 Duarte, C. M. and Krause-Jensen, D.: Export from Seagrass Meadows Contributes to Marine
791 Carbon Sequestration, Frontiers in Marine Science, 4,
792 https://doi.org/10.3389/fmars.2017.00013, 2017.
793 Duarte, C. M., Sintes, T., and Marbà, N.: Assessing the CO2 capture potential of seagrass
794 restoration projects, J. Appl. Ecol., 50, 1341-1349, https://doi.org/10.1111/1365-2664.12155,
795 2013.
796 Duarte, C. M., Marbà, N., Gacia, E., Fourqurean, J. W., Beggins, J., Barron, C., and Apostolaki,
797 E. T.: Seagrass community metabolism: Assessing the carbon sink capacity of seagrass
798 meadows, Global Biogeochemical Cycles, 24, 8, https://doi.org/10.1029/2010gb003793, 2010.
799 Duffy, J. E., Godwin, C. M., and Cardinale, B. J.: Biodiversity effects in the wild are common
800 and as strong as key drivers of productivity, Nature, 549, 261-264,
801 https://doi.org/10.1038/nature23886, 2017.
802 Enríquez, S., Agustí, S., and Duarte, C. M.: Light absorption by marine macrophytes,
803 Oecologia, 98, 121-129, https://doi.org/10.1007/BF00341462, 1994.
804 Faulwetter, S., Markantonatou, V., Pavloudi, C., Papageorgiou, N., Keklikoglou, K.,
805 Chatzinikolaou, E., Pafilis, E., Chatzigeorgiou, G., Vasileiadou, K., Dailianis, T., Fanini, L.,
806 Koulouri, P., and Arvanitidis, C.: Polytraits: A database on biological traits of marine
807 polychaetes, Biodiversity Data Journal, 2, e1024, https://doi.org/10.3897/BDJ.2.e1024, 2014.
808 Fenchel, T. and Glud, R. N.: Benthic primary production and O2-CO2 dynamics in a shallow-
809 water sediment: Spatial and temporal heterogeneity, Ophelia, 53, 159-171,
810 https://doi.org/10.1080/00785236.2000.10409446, 2000.
811 Frederiksen, M. S. and Glud, R. N.: Oxygen dynamics in the rhizosphere of Zostera marina: A
812 two-dimensional planar optode study, Limnology and Oceanography, 51, 1072-1083,
813 https://doi.org/10.4319/lo.2006.51.2.1072 2006.

https://doi.org/10.5194/bg-2023-173
Preprint. Discussion started: 4 October 2023

814 Gagnon, K., Bocoum, E.-H., Chen, C. Y., Baden, S. P., Moksnes, P.-O., and Infantes, E.: Rapid
815 faunal colonization and recovery of biodiversity and functional diversity following eelgrass
816 restoration, Restor. Ecol., 31, e13887, https://doi.org/10.1111/rec.13887, 2023.
817 Gamfeldt, L., Lefcheck, J. S., Byrnes, J. E. K., Cardinale, B. J., Duffy, J. E., and Griffin, J. N.:
818 Marine biodiversity and ecosystem functioning: what's known and what's next?, Oikos, 124,
819 252-265, https://doi.org/10.1111/oik.01549, 2015.
820 Gattuso, J.-P., Epitalon, J.-M., Lavigne, H., and Orr, J. C.: seacarb: Seawater carbonate
821 chemistry. R package version 3.3. https://cran.r-project.org/web/packages/seacarb/index.html
822 [code], 2022.
823 Gattuso, J.-P., Magnan, A. K., Bopp, L., Cheung, W. W., Duarte, C. M., Hinkel, J., Mcleod,
824 E., Micheli, F., Oschlies, A., and Williamson, P.: Ocean solutions to address climate change
825 and its effects on marine ecosystems, Frontiers in Marine Science, 5, 337,
826 https://doi.org/0.3389/fmars.2018.00337, 2018.
827 Glud, R. N.: Oxygen dynamics of marine sediments, Mar. Biol. Res., 4, 243-289,
828 https://doi.org/10.1080/17451000801888726, 2008.
829 Gullström, M., Baden, S., and Lindegarth, M.: Spatial patterns and environmental correlates in
830 leaf-associated epifaunal assemblages of temperate seagrass (Zostera marina) meadows,
831 Marine Biology, 159, 413-425, https://doi.org/10.1007/s00227-011-1819-z, 2012.
832 Hannides, A. K., Glazer, B. T., and Sansone, F. J.: Extraction and quantification of
833 microphytobenthic Chl a within calcareous reef sands, Limnology and Oceanography:
834 Methods, 12, 126-138, https://doi.org/10.4319/lom.2014.12.126, 2014.
835 Hooper, D. U., Chapin, F., Ewel, J., Hector, A., Inchausti, P., Lavorel, S., Lawton, J., Lodge,
836 D., Loreau, M., and Naeem, S.: Effects of biodiversity on ecosystem functioning: a consensus
837 of current knowledge, Ecological monographs, 75, 3-35, 2005.
838 Huang, Y.-H., Lee, C.-L., Chung, C.-Y., Hsiao, S.-C., and Lin, H.-J.: Carbon budgets of
839 multispecies seagrass beds at Dongsha Island in the South China Sea, Mar. Environ. Res., 106,
840 92-102, https://doi.org/10.1016/j.marenvres.2015.03.004, 2015.
841 Huber, S., Hansen, L. B., Nielsen, L. T., Rasmussen, M. L., Sølvsteen, J., Berglund, J., Paz von
842 Friesen, C., Danbolt, M., Envall, M., Infantes, E., and Moksnes, P.: Novel approach to large-
843 scale monitoring of submerged aquatic vegetation: A nationwide example from Sweden,
844 Integrated Environmental Assessment and Management, 18, 909-920,
845 https://doi.org/10.1002/ieam.4493, 2022.
846 Hume, A. C., Berg, P., and McGlathery, K. J.: Dissolved oxygen fluxes and ecosystem
847 metabolism in an eelgrass (Zostera marina) meadow measured with the eddy correlation
848 technique, Limnology and Oceanography, 56, 86-96,
849 https://doi.org/10.4319/lo.2011.56.1.0086, 2011.
850 Infantes, E., Hoeks, S., Adams, M. P., van der Heide, T., van Katwijk, M. M., and Bouma, T.
851 J.: Seagrass roots strongly reduce cliff erosion rates in sandy sediments, Mar. Ecol.-Prog. Ser.,
852 700, 1-12, https://doi.org/10.3354/meps14196, 2022.
853 Invers, O., Zimmerman, R. C., Alberte, R. S., Pérez, M., and Romero, J.: Inorganic carbon
854 sources for seagrass photosynthesis: An experimental evaluation of bicarbonate use in species
855 inhabiting temperate waters, J. Exp. Mar. Biol. Ecol., 265, 203-217,
856 https://doi.org/10.1016/S0022-0981(01)00332-X, 2001.
857 Jassby, A. D. and Platt, T.: Mathematical formulation of the relationship between
858 photosynthesis and light for phytoplankton, Limnology and Oceanography, 21, 540-547,
859 https://doi.org/10.4319/lo.1976.21.4.0540, 1976.
860 Jensen, S. I., Kühl, M., Glud, R. N., Jørgensen, L. B., and Priemé, A.: Oxic microzones and
861 radial oxygen loss from roots of Zostera marina, Mar. Ecol.-Prog. Ser., 293, 49-58,
862 https://doi.org/10.3354/meps293049, 2005.

https://doi.org/10.5194/bg-2023-173
Preprint. Discussion started: 4 October 2023

863 Jost, L.: Entropy and diversity, Oikos, 113, 363-375, https://doi.org/10.1111/j.2006.0030-
864 1299.14714.x, 2006.
865 Jovanovic, Z., Pedersen, M. Ø., Larsen, M., Kristensen, E., and Glud, R. N.: Rhizosphere O2
866 dynamics in young Zostera marina and Ruppia maritima, Mar. Ecol.-Prog. Ser., 518, 95-105,
867 https://doi.org/10.3354/meps11041, 2015.
868 Kindeberg, T., Severinson, J., and Carlsson, P.: Eelgrass meadows harbor more macrofaunal
869 species but bare sediments can be as functionally diverse, J. Exp. Mar. Biol. Ecol., 554, 151777,
870 https://doi.org/10.1016/j.jembe.2022.151777, 2022.
871 Kristensen, E.: Decomposition of macroalgae, vascular plants and sediment detritus in
872 seawater: Use of stepwise thermogravimetry, Biogeochemistry, 26, 1-24,
873 https://doi.org/10.1007/BF02180401, 1994.
874 Kristensen, E., Penha-Lopes, G., Delefosse, M., Valdemarsen, T., Quintana, C. O., and Banta,
875 G. T.: What is bioturbation? The need for a precise definition for fauna in aquatic sciences,
876 Mar. Ecol.-Prog. Ser., 446, 285-302, https://doi.org/10.3354/meps09506, 2012.
877 Laliberté, E. and Legendre, P.: A distance-based framework for measuring functional diversity
878 from multiple traits, Ecology, 91, 299-305, https://doi.org/10.1890/08-2244.1, 2010.
879 Larsson, C. and Axelsson, L.: Bicarbonate uptake and utilization in marine macroalgae,
880 European Journal of Phycology, 34, 79-86, https://doi.org/10.1080/09670269910001736112,
881 1999.
882 Long, M. H., Rheuban, J. E., McCorkle, D. C., Burdige, D. J., and Zimmerman, R. C.: Closing
883 the oxygen mass balance in shallow coastal ecosystems, Limnology and Oceanography, 0,
884 https://doi.org/10.1002/lno.11248, 2019.
885 Loreau, M. and Hector, A.: Partitioning selection and complementarity in biodiversity
886 experiments, Nature, 412, 72-76, https://doi.org/10.1038/35083573, 2001.
887 Lüdecke, D., Makowski, D., Waggoner, P., and Patil, I.: Performance: Assessment of
888 regression models performance, R package version 0.4, 5, 2020.
889 Lueker, T. J., Dickson, A. G., and Keeling, C. D.: Ocean pCO(2) calculated from dissolved
890 inorganic carbon, alkalinity, and equations for K-1 and K-2: validation based on laboratory
891 measurements of CO2 in gas and seawater at equilibrium, Marine Chemistry, 70, 105-119,
892 https://doi.org/10.1016/s0304-4203(00)00022-0, 2000.
893 The Marine Life Information Network: www.marlin.ac.uk, last access: 2022-10-15.
894 Mason, N. W., Mouillot, D., Lee, W. G., and Wilson, J. B.: Functional richness, functional
895 evenness and functional divergence: the primary components of functional diversity, Oikos,
896 111, 112-118, https://doi.org/10.1111/j.0030-1299.2005.13886.x, 2005.
897 McGinnis, D. F., Sommer, S., Lorke, A., Glud, R. N., and Linke, P.: Quantifying tidally driven
898 benthic oxygen exchange across permeable sediments: An aquatic eddy correlation study,
899 Journal of Geophysical Research: Oceans, 119, 6918-6932,
900 https://doi.org/10.1002/2014JC010303, 2014.
901 McGlathery, K. J., Reynolds, L. K., Cole, L. W., Orth, R. J., Marion, S. R., and Schwarzschild,
902 A.: Recovery trajectories during state change from bare sediment to eelgrass dominance, Mar.
903 Ecol.-Prog. Ser., 448, 209-221, https://doi.org/10.3354/meps09574, 2012.
904 McKenzie, L. J., Nordlund, L. M., Jones, B. L., Cullen-Unsworth, L. C., Roelfsema, C., and
905 Unsworth, R. K.: The global distribution of seagrass meadows, Environmental Research
906 Letters, 074041, https://doi.org/10.1088/1748-9326/ab7d06, 2020.
907 Moksnes, P.-O., Eriander, L., Infantes, E., and Holmer, M.: Local Regime Shifts Prevent
908 Natural Recovery and Restoration of Lost Eelgrass Beds Along the Swedish West Coast,
909 Estuaries Coasts, 1-20, https://doi.org/10.1007/s12237-018-0382-y, 2018.
910 Oksanen, J., Blanchet, G., Friendly, M., Klindt, R., Legendre, P., McGlinn, D., Minchin, P.,
911 O'Hara, G., Simpson, G., Solymos, P., Stevens, H., Szoecs, E., and Wagner, H.: vegan:

https://doi.org/10.5194/bg-2023-173
Preprint. Discussion started: 4 October 2023

912 Community Ecology Package R. https://cran.r-project.org/web/packages/vegan/index.html
913 [code], 2019.
914 Olsson, J., Toth, G. B., and Albers, E.: Biochemical composition of red, green and brown
915 seaweeds on the Swedish west coast, J. Appl. Phycol., 32, 3305-3317,
916 https://doi.org/10.1007/s10811-020-02145-w, 2020.
917 Orth, R. J., Lefcheck, J. S., McGlathery, K. S., Aoki, L., Luckenbach, M. W., Moore, K. A.,
918 Oreska, M. P. J., Snyder, R., Wilcox, D. J., and Lusk, B.: Restoration of seagrass habitat leads
919 to rapid recovery of coastal ecosystem services, Science Advances, 6, eabc6434,
920 https://doi.org/10.1126/sciadv.abc6434, 2020.
921 Österling, M. and Pihl, L.: Effects of filamentous green algal mats on benthic macrofaunal
922 functional feeding groups, J. Exp. Mar. Biol. Ecol., 263, 159-183,
923 https://doi.org/10.1016/S0022-0981(01)00304-5, 2001.
924 Ouisse, V., Migné, A., and Davoult, D.: Comparative study of methodologies to measure in
925 situ the intertidal benthic community metabolism during immersion, Estuarine, coastal and
926 shelf science, 136, 19-25, https://doi.org/10.1016/j.ecss.2013.10.032, 2014.
927 Penhale, P. A. and Smith, W. O.: Excretion of dissolved organic carbon by eelgrass (Zostera
928 marina) and its epiphytes, Limnology and Oceanography, 22, 400-407,
929 https://doi.org/10.4319/lo.1977.22.3.0400, 1977.
930 Pinardi, M., Bartoli, M., Longhi, D., Marzocchi, U., Laini, A., Ribaudo, C., and Viaroli, P.:
931 Benthic metabolism and denitrification in a river reach: a comparison between vegetated and
932 bare sediments, Journal of Limnology, 68, 133-145, https://doi.org/10.4081/jlimnol.2009.133,
933 2009.
934 Platt, T., Gallegos, C. L., and Harrison, W. G.: Photoinhibition of photosynthesis in natural
935 assemblages of marine phytoplankton, Journal of Marine Research, 38, 687-701, 1980.
936 Polsenaere, P., Deflandre, B., Thouzeau, G., Rigaud, S., Cox, T., Amice, E., Bec, T. L.,
937 Bihannic, I., and Maire, O.: Comparison of benthic oxygen exchange measured by aquatic
938 Eddy Covariance and Benthic Chambers in two contrasting coastal biotopes (Bay of Brest,
939 France), Regional Studies in Marine Science, 43, 101668,
940 https://doi.org/10.1016/j.rsma.2021.101668, 2021.
941 Queirós, A. M., Birchenough, S. N., Bremner, J., Godbold, J. A., Parker, R. E., Romero-
942 Ramirez, A., Reiss, H., Solan, M., Somerfield, P. J., and Van Colen, C.: A bioturbation
943 classification of European marine infaunal invertebrates, Ecology and evolution, 3, 3958-3985,
944 https://doi.org/10.1002/ece3.769, 2013.
945 RCoreTeam: R: A Language and Environment for Statistical Computing, R Foundation for
946 Statistical Computing [code], 2023.
947 Remy, F., Michel, L. N., Mascart, T., De Troch, M., and Lepoint, G.: Trophic ecology of
948 macrofauna inhabiting seagrass litter accumulations is related to the pulses of dead leaves,
949 Estuarine, Coastal and Shelf Science, 252, 107300,
950 https://doi.org/10.1016/j.ecss.2021.107300, 2021.
951 Rheuban, J. E., Berg, P., and McGlathery, K. J.: Ecosystem metabolism along a colonization
952 gradient of eelgrass (Zostera marina) measured by eddy correlation, Limnology and
953 Oceanography, 59, 1376-1387, https://doi.org/10.4319/lo.2014.59.4.1376, 2014a.
954 Rheuban, J. E., Berg, P., and McGlathery, K. J.: Multiple timescale processes drive ecosystem
955 metabolism in eelgrass (Zostera marina) meadows, Mar. Ecol.-Prog. Ser., 507, 1-13,
956 https://doi.org/10.3354/meps10843 2014b.
957 Ribaudo, C., Bartoli, M., Racchetti, E., Longhi, D., and Viaroli, P.: Seasonal fluxes of O2, DIC
958 and CH4 in sediments with Vallisneria spiralis: indications for radial oxygen loss, Aquat. Bot.,
959 94, 134-142, https://doi.org/10.1016/j.aquabot.2011.01.003, 2011.
960 Riera, R., Vasconcelos, J., Baden, S., Gerhardt, L., Sousa, R., and Infantes, E.: Severe shifts of
961 Zostera marina epifauna: Comparative study between 1997 and 2018 on the Swedish Skagerrak

https://doi.org/10.5194/bg-2023-173
Preprint. Discussion started: 4 October 2023

962 coast, Marine Pollution Bulletin, 158, 111434,
963 https://doi.org/10.1016/j.marpolbul.2020.111434, 2020.
964 Rodil, I. F., Attard, K. M., Gustafsson, C., and Norkko, A.: Variable contributions of seafloor
965 communities to ecosystem metabolism across a gradient of habitat-forming species, Mar.
966 Environ. Res., 105321, https://doi.org/10.1016/j.marenvres.2021.105321, 2021.
967 Rodil, I. F., Attard, K. M., Norkko, J., Glud, R. N., and Norkko, A.: Towards a sampling design
968 for characterizing habitat-specific benthic biodiversity related to oxygen flux dynamics using
969 Aquatic Eddy Covariance, PloS one, 14, e0211673,
970 https://doi.org/10.1371/journal.pone.0211673, 2019a.
971 Rodil, I. F., Attard, K. M., Norkko, J., Glud, R. N., and Norkko, A.: Estimating Respiration
972 Rates and Secondary Production of Macrobenthic Communities Across Coastal Habitats with
973 Contrasting Structural Biodiversity, Ecosystems, https://doi.org/10.1007/s10021-019-00427-
974 0, 2019b.
975 Smith, S. V. and Hollibaugh, J. T.: Coastal metabolism and the oceanic organic carbon balance,
976 Rev. Geophys., 31, 75-89, https://doi.org/10.1029/92rg02584, 1993.
977 Smith, S. V. and Key, G. S.: Carbon dioxide and metabolism in marine environments,
978 Limnology and Oceanography, 20, 493-495, https://doi.org/10.4319/lo.1975.20.3.0493, 1975.
979 Steinfurth, R. C., Lange, T., Oncken, N. S., Kristensen, E., Quintana, C. O., and Flindt, M. R.:
980 Improved benthic fauna community parameters after large-scale eelgrass (Zostera marina)
981 restoration in Horsens Fjord, Denmark, Mar. Ecol.-Prog. Ser., 687, 65-77,
982 https://doi.org/10.3354/meps14007, 2022.
983 Tait, L. W. and Schiel, D. R.: Dynamics of productivity in naturally structured macroalgal
984 assemblages: importance of canopy structure on light-use efficiency, Mar. Ecol.-Prog. Ser.,
985 421, 97-107, https://doi.org/10.3354/meps08909, 2011.
986 Tait, L. W., Hawes, I., and Schiel, D. R.: Shining Light on Benthic Macroalgae: Mechanisms
987 of Complementarity in Layered Macroalgal Assemblages, PLOS ONE, 9, e114146,
988 https://doi.org/10.1371/journal.pone.0114146, 2014.
989 Tang, M. and Kristensen, E.: Impact of microphytobenthos and macroinfauna on temporal
990 variation of benthic metabolism in shallow coastal sediments, J. Exp. Mar. Biol. Ecol., 349,
991 99-112, https://doi.org/10.1016/j.jembe.2007.05.011, 2007.
992 Thomson, A. C. G., Kristensen, E., Valdemarsen, T., and Quintana, C. O.: Short-term fate of
993 seagrass and macroalgal detritus in Arenicola marina bioturbated sediments, Mar. Ecol.-Prog.
994 Ser., 639, 21-35, https://doi.org/10.3354/meps13281 2020.
995 Tilman, D., Isbell, F., and Cowles, J. M.: Biodiversity and Ecosystem Functioning, Annual
996 Review of Ecology, Evolution, and Systematics, 45, 471-493, https://doi.org/10.1146/annurev-
997 ecolsys-120213-091917, 2014.
998 Törnroos, A. and Bonsdorff, E.: Developing the multitrait concept for functional diversity:
999 lessons from a system rich in functions but poor in species, Ecological Applications, 22, 2221-
1000 2236, https://doi.org/10.1890/11-2042.1, 2012.
1001 Trentman, M. T., Hall Jr., R. O., and Valett, H. M.: Exploring the mismatch between the theory
1002 and application of photosynthetic quotients in aquatic ecosystems, Limnology and
1003 Oceanography Letters, 8, 565-579, https://doi.org/10.1002/lol2.10326, 2023.
1004 Turk, D., Yates, K. K., Vega-Rodriguez, M., Toro-Farmer, G., L'Esperance, C., Melo, N.,
1005 Ramsewak, D., Dowd, M., Estrada, S. C., Muller-Karger, F. E., Herwitz, S. R., and McGillis,
1006 W. R.: Community metabolism in shallow coral reef and seagrass ecosystems, lower Florida
1007 Keys, Mar. Ecol.-Prog. Ser., 538, 35-52, https://doi.org/10.3354/meps11385, 2015.
1008 Unsworth, R. K. F., Cullen-Unsworth, L. C., Jones, B. L. H., and Lilley, R. J.: The planetary
1009 role of seagrass conservation, Science, 377, 609-613, https://doi.org/10.1126/science.abq6923,
1010 2022.

https://doi.org/10.5194/bg-2023-173
Preprint. Discussion started: 4 October 2023

1011 Van Dam, B. R., Lopes, C., Osburn, C. L., and Fourqurean, J. W.: Net heterotrophy and
1012 carbonate dissolution in two subtropical seagrass meadows, Biogeosciences, 16, 4411-4428,
1013 https://doi.org/10.5194/bg-16-4411-2019, 2019.
1014 Villéger, S., Mason, N. W., and Mouillot, D.: New multidimensional functional diversity
1015 indices for a multifaceted framework in functional ecology, Ecology, 89, 2290-2301,
1016 https://doi.org/10.1890/07-1206.1, 2008.
1017 Ward, M., Kindinger, T. L., Hirsh, H. K., Hill, T. M., Jellison, B. M., Lummis, S., Rivest, E.
1018 B., Waldbusser, G. G., Gaylord, B., and Kroeker, K. J.: Reviews and syntheses: Spatial and
1019 temporal patterns in seagrass metabolic fluxes, Biogeosciences, 19, 689-699,
1020 https://doi.org/10.5194/bg-19-689-2022, 2022.
1021 Waycott, M., Duarte, C. M., Carruthers, T. J. B., Orth, R. J., Dennison, W. C., Olyarnik, S.,
1022 Calladine, A., Fourqurean, J. W., Heck, K. L., Hughes, A., Kendrick, G. A., Kenworthy, W.,
1023 Short, F. T., and Williams, S. L.: Accelerating loss of seagrasses across the globe threatens
1024 coastal ecosystems, Proceedings of the National Academy of Sciences, USA, 106, 12377-
1025 12381, https://doi.org/10.1073/pnas.0905620106, 2009.
1026 Weiss, R.: The solubility of nitrogen, oxygen and argon in water and seawater, Deep sea
1027 research and oceanographic abstracts, 721-735, https://doi.org/10.1016/0011-7471(70)90037-
1028 9,
1029 Wijsman, J. W. M., Herman, P. M. J., and Gomoiu, M.-T.: Spatial distribution in sediment
1030 characteristics and benthic activity on the northwestern Black Sea shelf, Mar. Ecol.-Prog. Ser.,
1031 181, 25-39, http://dx.doi.org/10.3354/meps181025, 1999.
1032 Zimmerman, R. C.: A biooptical model of irradiance distribution and photosynthesis in
1033 seagrass canopies, Limnology and Oceanography, 48, 568-585,
1034 https://doi.org/10.4319/lo.2003.48.1_part_2.0568, 2003.
1035